Policy Research Working Paper 10400

Detox Development: Repurposing Environmentally Harmful Subsidies

Background Paper

People's Unequal Exposure to Air Pollution

Evidence for the World's Coal-Fired Power Plants

Xinming Du
Jun Rentschler
Jason Russ

WORLD BANK GROUP
Sustainable Development Practice Group
Office of the Chief Economist
April 2023

Policy Research Working Paper 10400

Abstract

The world's over 3,800 coal-fired power plants are sources of substantial emissions of toxic air pollutants. This study explores people's unequal exposure to air pollution from these coal plants. It simulates the wind dispersion of pollutants originating from each coal power plant using the Hybrid Single Particle Lagrangian Integrated Trajectory Model (HYSPLIT) with Gaussian dispersion. The study generates three-dimensional pollution trajectories and provide a global map of nitrogen oxide (NOx), sulfur dioxide (SO2), and particle pollution from coal plants and their contributions to overall pollution levels. The study estimates that 2.3 billion people globally are exposed to SO2 and particle pollution from coal plants; 247.5 million of them are exposed to transboundary pollution from foreign coal plants. The findings show that pollution increases with income levels, though at a diminishing rate at high income levels. In the proximity of coal power plants, downwind areas are associated with higher pollution and lower income levels compared to areas upwind. These findings are consistent with strategic location choices that cause or reinforce environmental injustices associated with air pollution.

This paper is a product of the Office of the Chief Economist, Sustainable Development Practice Group. It is part of a larger effort by the World Bank to provide open access to its research and make a contribution to development policy discussions around the world. Policy Research Working Papers are also posted on the Web at http://www.worldbank.org/prwp. The authors may be contacted at xd2197@columbia.edu, jrentschler@worldbank.org, and jruss@worldbank.org.

People's Unequal Exposure to Air Pollution: Evidence for the World's Coal-Fired Power Plants

Xinming Du, Jun Rentschler, Jason Russ*

Keywords: Air pollution, coal power, environmental justice

JEL codes: Q50, Q56, O44, D63

Topics: Air pollution, Power sector economics, Environmental Policies and Institutions

Acknowledgements: The authors thank Esteban Balseca, Richard Damania, Kichan Kim, and Christoph Klaiber for valuable feedback on an earlier draft of this study. This study is a technical background paper to the World Bank flagship report "Detox Development: Repurposing environmentally harmful subsidies" (2023).

*Du: Columbia University, xd2197@columbia.edu; Rentschler: The World Bank, jrentschler@worldbank.org; Russ: The World Bank, jruss@worldbank.org

1 Introduction

Coal remains a widely used source of energy supply, but is associated with tremendous societal costs, including air pollution, climate change, acid rain, wastewater discharge, and wastage of financial resources. In the U.S. alone, coal-fired power plants release more than 3.1 million tons of sulfur dioxide (SO_2), 1.5 million tons of nitrogen oxide (NO_x), and 0.2 million tons of particulate matter each year.[1] At the same time, they also release substantial lead, mercury, volatile organic compounds, arsenic, and other toxic chemicals. The evidence is unequivocal that these air pollutants are linked with heightened risks of asthma, cancer, heart and lung ailments, neurological diseases, and broader public health impacts (Manisalidis et al., 2020).

In addition to their high environmental and health costs, coal-fired power plants operate with low efficiency and a lack of profitability. More than 40 percent of the world's coal plants are operating at a loss, not least due to high fuel costs, and this share could rise to 75 percent by 2040 (Gray et al., 2018). However, power plants are still expanding in number and capacity, as their economic viability is propped up by fossil fuel subsidies. Each year, the IMF estimates that governments around the world spend around $13.6 billion to artificially lower the price of coal, thus perpetuating the operation of unprofitable coal-fired power plants and the associated air pollution (Parry et al., 2021).

The existing literature, primarily focused on the U.S., has documented significant and systematic inequality in the exposure to such air pollution. For instance, hazardous waste facilities are disproportionately sited in minority communities (Boer et al., 1997; Graham et al., 1999). Analyzing environmental justice in the fossil fuel industry, Carpenter and Wagner (2019) find that air pollution is higher in counties with higher unemployment levels. This pattern is inconsistent with the fair treatment notion of the U.S. Environmental Protection Agency (EPA), which states that "no group of people should bear a disproportionate share of the negative environmental consequences resulting from industrial, governmental and commercial operations or policies" (EPA, 2020). While such environmental injustice in the context of air pollution is well documented in high-income countries, evidence remains scarce for lower income countries and at the global scale.

This paper addresses this gap by documenting the regressive nature of the air pollution and health burden associated with the continued use of coal power plants. It finds that, globally, 2.32 billion people are exposed to air pollution originating from coal power plants. We find that air pollution from coal plants increases with income levels, though at a diminishing rate at high income levels. In other words, coal power plants are located in richer countries, and richer

[1] Data comes from the 2014 National Emissions Inventory (NEI) compiled by the U.S. EPA.

regions within countries.

However, in the proximity of plants, downwind areas are associated with higher pollution and lower income levels compared to areas upwind; thus suggesting that low-income groups are disproportionately affected by air pollution. This result is consistent with strategic location choices for polluting assets, and the spatial sorting of low- and high-income communities. It is indicative of systematic environmental injustice concerns at a global scale.

2 Evidence from the existing literature

Economic development has been associated with an increase in polluting activities.

There is some evidence that as countries develop economically, they tend to consume more energy and expand industrial activities – thus resulting in higher economic outputs and more pollution. Eventually, however, polluting activities are replaced by cleaner ones (e.g. sectoral switch from industry to services), and polluting technologies may be replaced by cleaner options (e.g. replacing coal with gas or renewables). Rentschler and Leonova (2022) find that air pollution is the most severe in medium-income countries, and is lower in both low- and high-income countries.

Polluting assets are purposefully located in low-income or minority neighbourhoods. Wolverton (2009) examines the role of community socioeconomic characteristics at the time of location decisions of manufacturing plants, while controlling for other input costs. They show that the presence of racial minority communities is significantly and positively related to plant location, while income is significantly and negatively related to plant location. There is some evidence that both very poor and very rich neighborhoods have fewer polluting facilities (Been and Gupta, 1997; Arora and Cason, 1999). Zwickl et al. (2014) examine U.S. cities' environmental inequality by race in 2007, and find that Black and Hispanic neighborhoods are the most exposed groups to industrial air toxics in the Midwest and South Central regions. A descriptive analysis for the period from 1995 to 2004 shows that Black communities have remained consistently more exposed to air pollution than white communities. They show that income is non-linearly correlated with pollution exposure: middle-class African-Americans are exposed to more toxins than lower-income white communities.

Pollution transcends borders. Studies have shown that polluting sites can display a systematic tendency to be located near administrative borders. This may reduce environmental and health costs on domestic residents, while creating transboundary externalities. Monogan III et al. (2017) provides empirical evidence that major air polluters in the U.S. are more likely to be located near the downwind borders of states. Similarly, Morehouse and Rubin (2021) show

that coal-fired electricity generators in the U.S. tend to locate near county and state borders; 57 percent are within 5 kilometers of a county border; 25 percent are within 5 kilometers of a state border. In comparison, natural gas plants – which have substantially lower emissions and face lower emission-based environmental regulatory pressures – do not exhibit this spatial sorting pattern. The presence of environmental free-riding has also been detected in cases of water pollution disproportionately borne by downstream jurisdictions (Sigman, 2005; Lipscomb and Mobarak, 2016) and in toxic emissions into the air and water near state borders relative to same-state regions (Helland and Whitford, 2003).

Air pollution can suppress socioeconomic development, and alter the socioeconomic composition of neighborhoods. Hanlon (2019) shows that pollution due to coal had negative impacts on city growth in Britain in 1851-1911, measured by low employment and slow population growth. Heblich et al. (2021) show that air pollution has historically been unequally distributed across neighborhoods within former industrial cities, which has led to persistent sorting across neighborhoods by socioeconomic status. Poorer households tend to live downwind of pollution sources. Historic air pollution patterns are shown to explain up to 20 percent of observed neighborhood segregation in 2011, even though coal pollution stopped in the 1970s. Similarly, in China, Chen et al. (2022) show that air quality plays a role in migration choices of workers. Using a nationwide air quality reporting program as a natural experiment, the study finds that 1 percent of migration decisions are made in response to newly available information on air quality. Similar findings are documented by Khanna et al. (2021), who find that workers emigrate across cities within China when air quality deteriorates. The study also shows that skilled workers have more migration responses than the unskilled, and that air quality explains across-city differences in productivity.

Air pollution decreases labor productivity. To control for potential quantity responses to productivity changes, Graff Zivin and Neidell (2012) focus on production workers in busy farming seasons, whose contracts specify fixed working hours. They find that a 10 parts per billion (ppb) increase in ozone (O3) concentration decreases the labor productivity of US farmers by 5.5 percent. In a similar vein, Chang et al. (2019) study service workers in a call center where workers have little discretion over their work hours. They show that a 10 unit increase in an air pollution index reduces the number of calls workers complete by 0.35 percent.

To overcome the endogeneity issues, several studies adopt an instrumental variable approach to document similar adverse effects on productivity. He et al. (2019) take advantage of pollution spikes caused by atmospheric inversion, which occurs when hot air masses are caught above cold air masses, thus trapping pollutants. The study finds that a $10\mu g/m^3$ increase in $PM_{2.5}$

at least 25 days can reduce the daily output of manufacturing workers by 1 percent. Using the same instrument, Chen and Zhang (2021) show that a 10 unit increase in an air pollution index decreased the labor productivity of prison workers by 4 percent.

Air pollution has detrimental impacts on human health. To isolate the impact of air pollution on health outcomes, several studies have used prevailing wind directions as an identification instrument. Anderson (2019) leverage the quasi-random variation in pollution levels generated by wind patterns near highways in Los Angeles in 1999-2001. The study finds that doubling the percentage of time spent downwind of a highway increases mortality among individuals aged over 75 by 3.6 to 6.8 percent. Deryugina et al. (2019) study Medicare beneficiaries in the U.S. and find that a 1 $\mu g/m^3$ increase in $PM_{2.5}$ causes 0.69 additional deaths per million elderly individuals.

Other studies use atmospheric inversion as an instrument to study the impact of air pollution on health outcomes. Controlling for temperature, inversions do not represent a health risk apart from the heightened accumulation of pollutants that they cause. Arceo et al. (2016) show that an increase of 1 ppb in carbon monoxide (CO) and 1 $\mu g/m^3$ in PM_{10} during atmospheric inversions result in 0.032 and 2.4 additional infant deaths per million births.

The timing of environmental regulations and of polluting events can also help to identify health impacts. Greenstone and Hanna (2014) show that India's anti-pollution laws led to improvements in air quality and had positive but insignificant impacts on infant mortality. He et al. (2016) exploit the timing of mandated air quality measures during the 2008 Beijing Olympic Games, and find that a 10 percent decrease in PM_{10} concentrations reduced the monthly standardized all-cause mortality rate by 8 percent. Barrows et al. (2019) show that the expansion of coal-fired power generation increases surrounding NO_2 pollution. A one gigawatt increase in coal-fired power generation capacity is estimated to result in a 14 percent increase in infant mortality rates in districts near the plant site compared to more distant districts. Fan et al. (2020) apply a regression discontinuity design based on different starting dates of winter heating in different cities in China. They find that winter heating increased the weekly Air Quality Index[2] by 36 percent on average and caused a 14 percent increase in the all-cause mortality rate. Imelda (2018) studies the effect of an Indonesian kerosene to liquid petroleum gas (LPG) cook stove conversion program. LPG cook stoves produce significantly less indoor air pollution, which the study documents to lead to 0.4 fewer infant deaths per thousand births.

Air pollution increases private and public health expenditures. The health impacts of air pollution are not only documented in mortality and morbidity rates, but also in health ex-

[2]The Air Quality Index (AQI) in China is calculated based on six air pollutants, SO_2, NO_2, PM_{10}, $PM_{2.5}$, CO and O_3. A low value means good air quality, and a high value means poor air quality.

penditure and hospital visit numbers. In the U.S., each 1 $\mu g/m^3$ increase in $PM_{2.5}$ is estimated to increase three-day emergency room (ER) visits by 2.7 per million and inpatient ER spending by \$16,000 per million (Deryugina et al., 2019). Using weather variations for identification, Barwick et al. (2018) find that a 10 $\mu g/m^3$ decrease in $PM_{2.5}$ reduces annual healthcare spending by over \$9.2 billion in China, which is equivalent to 1.5 percent of average annual healthcare expenditure. Deschenes et al. (2017) estimate that NO_x and O_3 pollution levels dropped by 35 percent and 6 percent respectively after the NO_x Budget Trading Program started in participating states. As a result, drug expenditures decreased by 1.9 percent in participating states.

Schlenker and Walker (2015) use network delays to instrument air pollution at California airports. They find a one standard deviation increase in daily airplane taxi time increases CO pollution by 23 percent, and a one standard deviation increase in pollution explains one third of daily asthma admissions. Relying on a driving restriction policy, Zhong et al. (2017) find that a 22 percent increase in NO_2 due to traffic congestion increases ambulance calls by 12 percent in Beijing. Apart from direct medical expenditure, some studies also document increases in protective investments. For example, Ito and Zhang (2020) find that household spending on air purifiers increases by \$1.34 for each 1 $\mu g/m^3$ increase in PM_{10} due to the Huai River heating policy. A 100-point increase in AQI increases spending on all masks by 54.5 percent and anti-$PM_{2.5}$ masks by 70.6 percent (Zhang and Mu, 2018).

We make three contributions to the literature. First, studies on air pollution and its impacts primarily use wind directions to evaluate unequal exposure or instrument pollution. However, actual pollution disperses as a mass with changing directions along its pathways. We combine the HYSPLIT model and Gaussian dispersion to better simulate trajectories. Second, existing papers focus on one region or conduct program evaluations. Our paper analyzes all operating coal power plants worldwide and projects pollution on income maps. This practice provides a global picture of pollution and its coexistence with poverty. Third, while earlier evidence shows that pollution worsens labor productivity, there is no causal evidence that pollution affects aggregate economic outputs. We adopt econometric methods to test changes in GDP per capita, GDP, and HDI due to plant operations.

3 Data and methods

3.1 Data

In this study, we analyze air pollution originating from coal-fired power plants. Basic characteristics of coal plants are derived from the Global Coal Plant Tracker developed by CoalSwarm

(Shearer et al., 2021). The tracker uses public sources to identify and document all coal-fired power generation units with a capacity of at least 30 megawatts across the world. For each unit, it records the name, operator, capacity, coordinates, operating status, as well as start and end years (if applicable). To determine the sample for this study, we use coal plants that were operational in January 2013. This yields a sample of 6,321 coal-fired power generation units, sited in 3,875 unique plant locations. These plants are distributed widely across the world, though mainly concentrated in the U.S., Europe, and South and East Asia (Figure 1).

Figure 1: Power plant locations

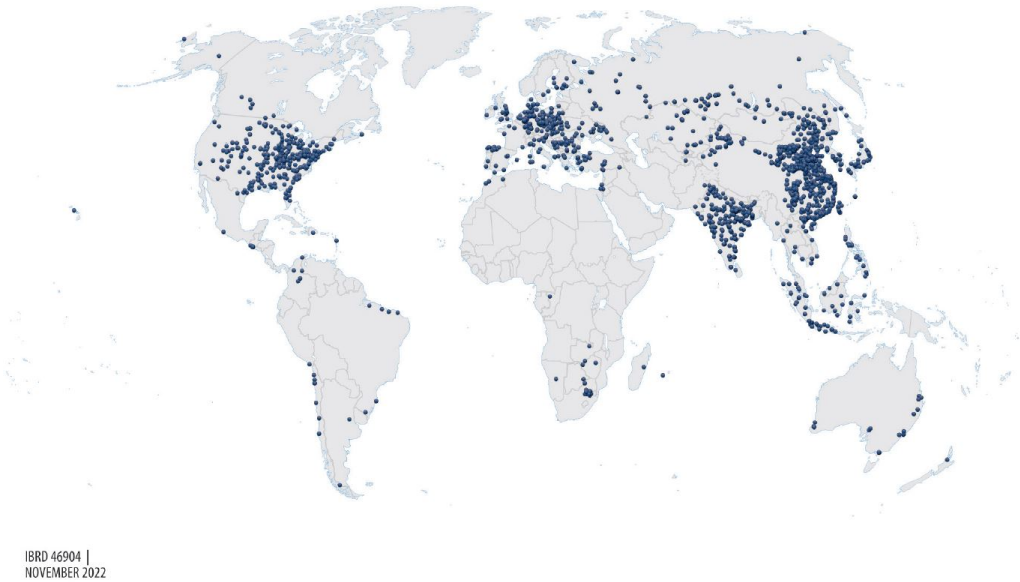

Notes: Source: (Shearer et al., 2021). This figure shows the spatial distribution of coal-fired power plants as of January 2013. Each black dot denotes an operating unit.

Emission intensities of power plants are obtained from the Global Power Emissions Database (GPED) (Tong et al., 2018). GPED records global fossil fuel- and biomass-fired power plants and their emissions as of 2010 at the plant level (Tong et al., 2018). It is compiled based on basic information from plant operators, complemented with emissions data for plants in the U.S., China, and India from more comprehensive data contained in the regional databases, the Emissions Generation Resource Integrated Database (eGRID) from the U.S. EPA, the China coal-fired Power plant Emissions Database (CPED) (Liu et al., 2015) and the Indian Coal-fired Power Plants Database (ICPD) (Lu and Streets, 2012). We use NO_x, SO_2, and primary particulate emission intensities at the plant level in 2010.

While GPED covers 231 countries and regions and all their coal-fired power generating units, it contains missing emission intensities, which we manually fill in using countrywide averages.

We also use population data to calculate pollution exposure. Population data comes from the

Gridded Population of the World (GPWv4) dataset, developed by Columbia University based on population and housing censuses (CIESIN, 2016).

Data are available in five-year steps for the period from 2000 to 2020 with a spatial resolution of 30 arc-seconds (which is equivalent to about 1 kilometer at the equator). We use the 2015 version for further analysis.

Income data is obtained from Kummu et al. (2018) who provide gridded global datasets for GDP, GDP per capita, and Human Development Index (HDI) for every year from 1990 to 2015. GDP and HDI estimates are provided at 5 arc-minutes resolution, while GDP per capita (PPP) has a resolution of 30 arc-seconds. To generate these datasets, Kummu et al. (2018) use World Bank datasets, the Central Intelligence Agency's (CIA) World Factbook, and subnational GDP per capita data developed by Gennaioli et al. (2012), and employ country-specific interpolation and extrapolation. These gridded datasets are consistent worldwide and comparable across countries and years. Figure 2 shows gridded GDP maps for six years. Areas that do not have any population are dropped from our analysis.

3.2 Model

We simulate the wind-dispersion of air pollutants from coal power plants in four steps.

First, we use the Hybrid Single Particle Lagrangian Integrated Trajectory Model (HYSPLIT) to simulate the movement trajectories of particles originating from power plants, in line with Du et al. (2020). We generate 96 forward trajectories for 6,321 power generation units. Four such trajectories are visualized in Figure 3. Pollutant movement is calculated based on the Global Data Assimilation System at a 1 arc-degree resolution. We assume each pollutant particle has a four-day (i.e. 96 hours) lifespan and an initial altitude of 100 meters. Starting from the originating plant, the location of particles is simulated beginning from 11 am on January 1st, 2013, in hourly increments until 11 am on January 5th. Each location is a three-dimensional coordinate, specifying longitude, latitude, and altitude.

The second step is to account for particle dispersion along the simulated trajectories. This reflects the fact that air pollution is not a single particle but an air mass, and the affected area is not a trajectory line but an area with a concentration gradient. Thus, we translate each simulated point location from the HYSPLIT modeling into an affected area. We follow the Calpuff model and simulate three-dimensional Gaussian dispersion along the modeled trajectories. Dispersion is specified as follows (Agency, 1995):

$$C = \frac{Q}{2\pi\sigma_x\sigma_y} g \; exp[\frac{-d_a^2}{2\sigma_x^2}] exp[\frac{-d_c^2}{2\sigma_y^2}]$$

Figure 2: Gridded GDP map

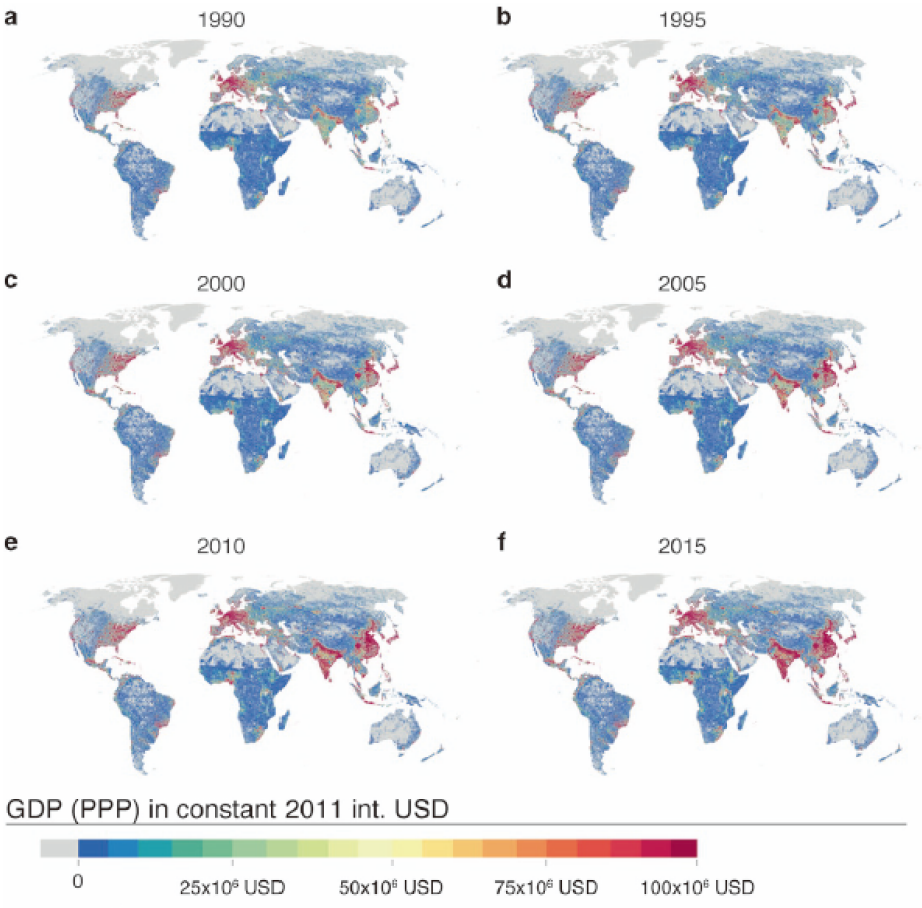

Notes: Source: (Kummu et al., 2018). This figure shows the temporal and spatial variation of GDP 1990-2015.

$$g = \frac{2}{\sqrt{2\pi}\sigma_z} \sum_{n=-\infty}^{\infty} exp[\frac{-(H_e + 2nh)^2}{2\sigma_z^2}]$$

where C is the pollution concentration of interest; Q is the pollutant mass, positively correlated with emission intensity; σ_x, σ_y, and σ_z are standard deviations of dispersion. These dispersion parameters are chosen based on Miller (1978) and actual weather conditions from the Global Data Assimilation System (Kleist et al., 2009). Moreover, d_x, d_y, and d_z are distances from the pollution source to the recipient in along-wind, cross-wind, and vertical directions; H_e and h measure the altitude of the pollution source and recipient respectively.

After translating the 606,816 location points (i.e. trajectories for 6,321 coal power generating units, each consisting of 96 hourly location points) into affected areas, we aggregate pollution concentrations at the recipient pixel level. At each recipient pixel i, the concentration is the sum of all power plants' contribution of emissions at each time step. Thus, at the steady state,

Figure 3: Four sample trajectories from HYSPLIT and pollution dispersion modeling output

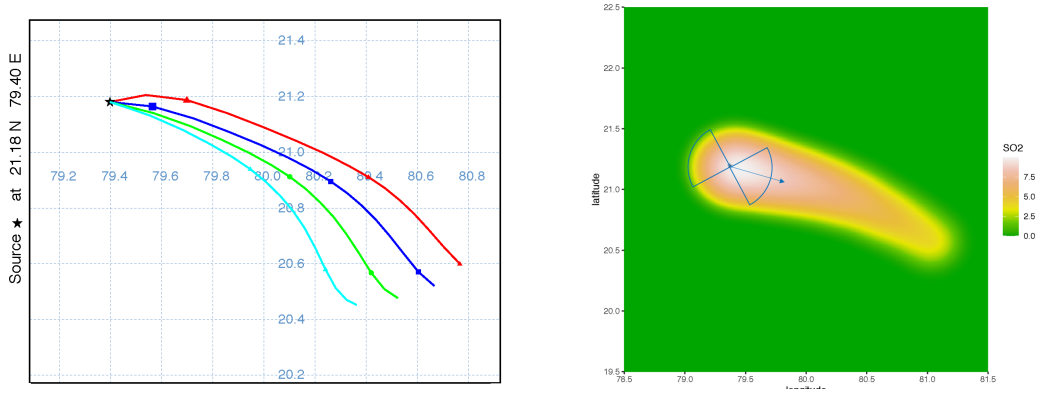

Notes: The left figure shows four sample trajectories from the Mauda power plant in India. Four simulated trajectories started at 5am, 11am, 5pm and 11pm on January 1st, 2013. The right figure shows our modeled outputs. Background color shows pollution concentrations. Blue dot and arrow show plant location and wind direction. Transparent blue quarter circles are borders of upwind and downwind areas analyzed in Section 4.3.

ambient pollution at any recipient pixel is calculated as:

$$Concentration_i = \sum_{a=0}^{\infty} \sum_{j=1}^{6{,}321} Pollution_{ija}$$

where $Pollution_{ija}$ captures pollution emitted by plant j received by pixel i, and pollutant is at age a. Based on hourly observations, we add two additional steps within each hour. In the actual dispersion, air pollutant disperses every second in each hour interval. Due to the computation limit, we only calculate dispersion every 20 minutes. Compared with hourly dispersion, this practice helps to capture affected areas within each hour.

The last step is to project income maps to the pollution map. Through steps 1 and 2, we generate pollution maps for SO_2, NO_x and primary particles[3] at 0.01-degree resolution. We focus on SO_2 in Section 4 as coal power plants contribute to most ambient SO_2 compared with other emission sources. Also, primary particles and NO_x are driven mainly by secondary formation, and HYSPLIT modeling cannot capture further chemical transformations.

Out of a total of 648,000,000 pixels in a world map at 0.01-degree resolution, only 1.72 percent of pixels are populated. We overlay pollution and population maps, and drop areas with zero population. This yields a final sample of 11,163,331 pixels at 0.01-degree resolution.

Figure 4 shows sample maps for simulated SO_2 pollution. The upper left figure shows

[3]Primary pollutants are pollutants emitted directly from a source. Secondary pollutants are not directly emitted but form when other primary pollutants react. Besides, particles include particles of all sizes.

pollution distribution near the Mauda coal power station in India. SO_2 concentrations decline as the pollutant mass moves further away from the plant. The other three figures show SO_2 pollution in India, China, and Europe. They document pollution hotspots near power plants and their surrounding areas, with concentrations decreasing with distances to plants. Besides, concentration levels differ across affected areas due to different emission intensities. For instance, coal plants in China and India can be seen to be more polluting compared to those in Poland.

Figure 4: Modeled SO_2 concentration maps for India, China, and Central Europe

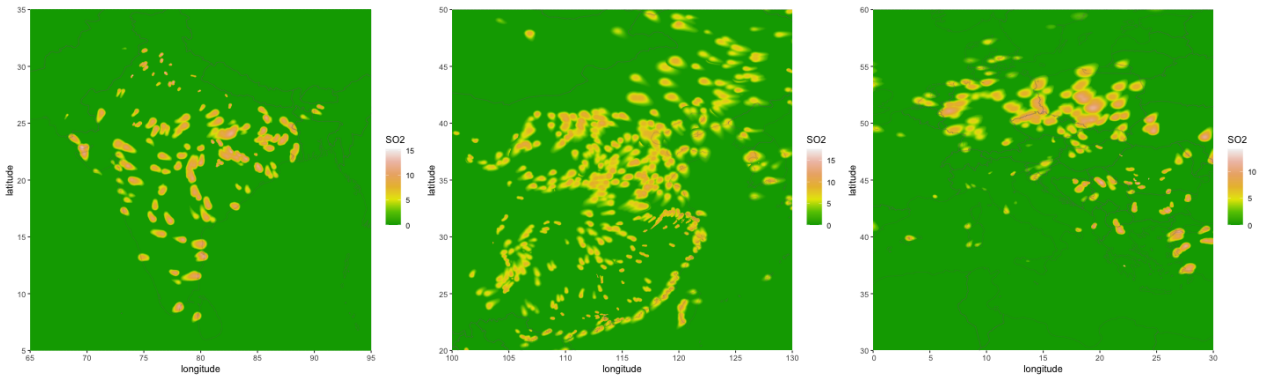

Notes: SO_2 distribution in India (left), China (middle), and Germany and Poland (right). Unit: ln(ng/m^3). Spatial resolution: 0.01 arc-degrees.

4 Findings: Exposure, health impacts, and the unequal burden of pollution

In this section, we first present a summary of the exposure and health impact estimates derived from the modeled air pollution maps. Our modeled results provide a global picture of the overall pollution contribution of coal power plants and its spatial distribution. We estimate that 2.32 billion people are exposed to particle pollution from coal power plants, with China and India together accounting for 1.29 billion.

We then present evidence on the unequal distribution of air pollution from coal plants. At the country level, we show that higher national income levels are associated with more coal-fired power plants, and thus higher pollution burdens. Similar patterns are found within countries, with negative associations between local income levels and air quality. We also show that power plant locations are not evenly distributed across income groups. In the proximity of coal plants, downwind areas are systematically poorer than upwind areas. Thus, poorer communities are disproportionately exposed to toxic pollution from coal plants.

4.1 Population exposed to power plants' emissions

Using the modeled air pollution map, we estimate global exposure headcounts to coal power plant pollution around the world. We estimate that globally 2.32 billion people are exposed to SO_2 emissions from coal-fired power plants, 1.29 billion of which are in China and India alone. Figure 5 shows the top 10 countries with the highest population and highest proportion of population affected by coal plants' pollution. China, India, and the U.S. have 895.7, 392.4, and 157.0 million people exposed respectively, due to their high plant concentrations and population densities. The left panel of Figure 7 visualizes the proportion of population that are exposed to any level of coal plants' pollution relative to national population in each country. Most countries show similar patterns as Figure 1 given within-country pollution dispersion. Czechia and Germany have 97 percent and 83 percent of their population exposed, including to high transboundary pollution flow from foreign plants. The proportion of affected population ranges from 0 to 97 percent, with an average of 12 percent; 13 countries have over half of their population exposed to air pollution from coal plants.

Focusing on cross-border pollutant flows, Figure 8 shows the share of national populations that are exposed to foreign plants' pollution (left) and that face higher foreign pollution than domestic pollution (right). Overall, 247.5 million people world-wide are exposed to transboundary air pollution from foreign coal plants. The top affected countries are shown in Figure 6. Transboundary pollution affects 24.1 percent of the population in Czechia, where Poland and Germany are the primary sources of transboundary flows.

Globally, 160 million people face SO_2 pollution from coal plants that exceed the World Health Organization (WHO) guideline value of 40 $\mu g/m^3$ – and this does not account for pollution from other sources. These WHO threshold values are evidence-informed quantitative recommendations based on a systematic review of the evidence of adverse health effects and dose-response functions. SO_2 of 40 $\mu g/m^3$ is the upper limit of the 24-hour mean. The proportion of population exposed to SO_2 over 40 $\mu g/m^3$ in each country is visualized in the right panel of Figure 7.

According to the WHO, 'achieving the recommended guideline levels will deliver substantial health benefits globally'.[4] This implies that even if other natural and anthropogenic pollution sources could be mitigated, coal-fired power plants alone are leading to substantial health risks for large population groups.

[4]Detailed explanations can be found on the WHO website: https://www.who.int/news-room/questions-and-answers/item/who-global-air-quality-guidelines

Figure 5: Top 10 countries with the highest population exposure to coal power plant pollution, in absolute terms (left) and as a share of population (right)

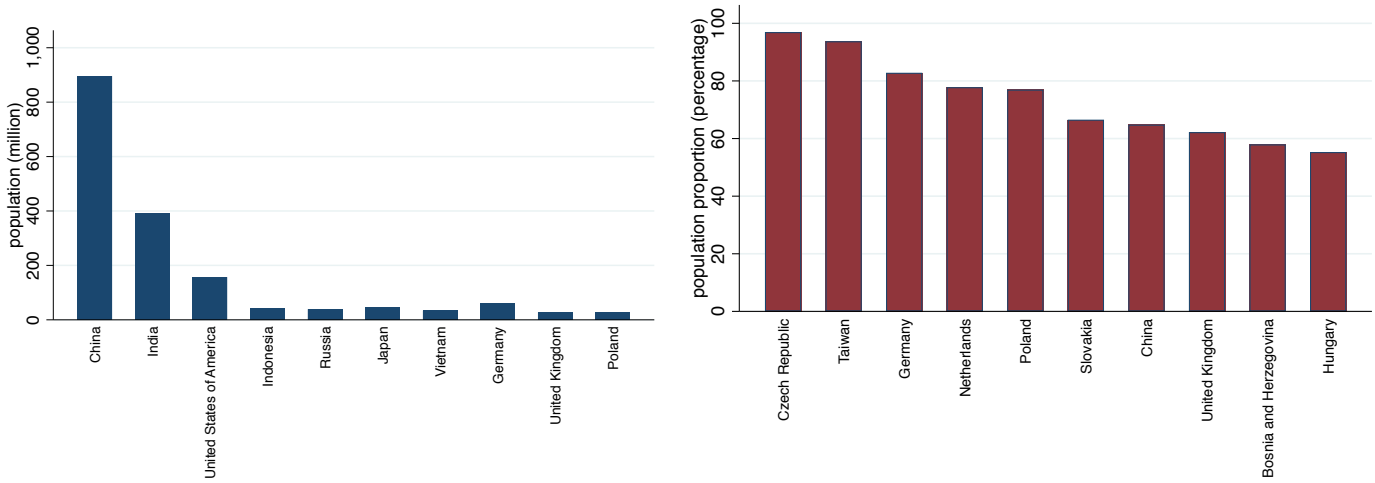

Notes: The left figure shows population in absolute values that are exposed to any level of power plants' pollution. The right figure shows the proportion of population exposed to any level of power plants' pollution.

Figure 6: Top 10 countries with the highest population and the highest proportion of population exposed to transboundary pollution

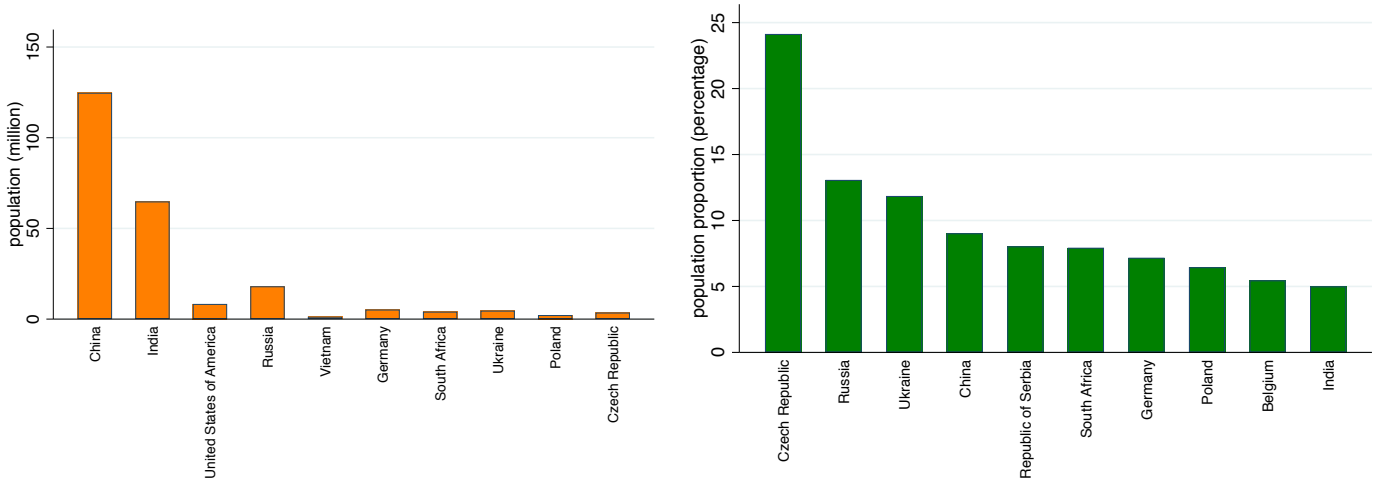

Notes: The left figure shows population in absolute values that are exposed to any level of foreign power plants' transboundary pollution. The right figure shows the proportion of population exposed to any level of foreign power plants' transboundary pollution.

4.2 Coal-fired air pollution at different national income levels

In this section, we show that exposure to air pollution from coal power plants varies significantly by income levels. At the country level, we show that higher national income levels are associated

Figure 7: Population exposed to power plant pollution

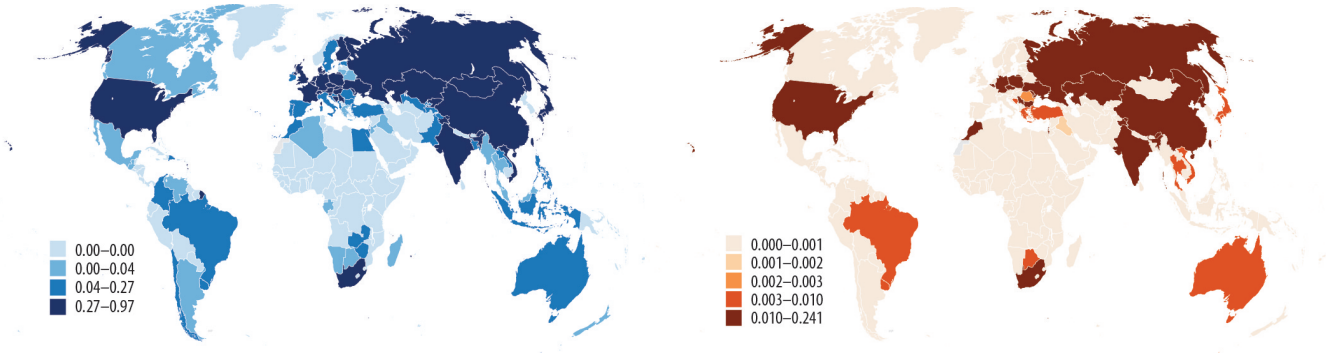

Notes: The left figure shows the proportion of population in each country exposed to any level of power plant pollution exposure. The right figure shows the proportion of population exposed to unhealthy levels of air pollution.

Figure 8: Population exposed to transboundary pollution

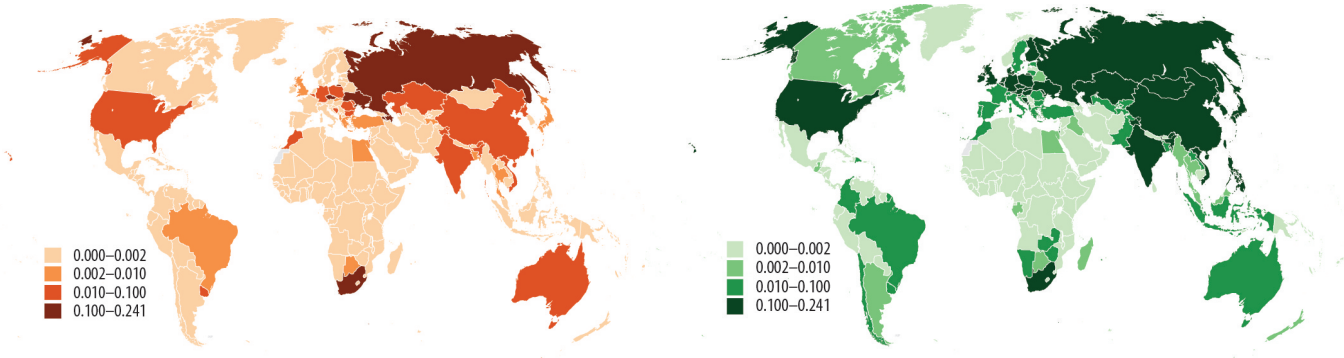

Notes: The left figure shows the proportion of population in each country exposed to any level of foreign power plants' transboundary pollution exposure. The right figure shows the proportion of population exposed to higher transboundary pollution than domestic pollution.

with more coal-fired power plants, and thus higher pollution burdens. Similar patterns are found within countries, with negative associations between local income levels and air quality. More flexible fittings show a concave function, suggesting that air pollution from coal plants increases in line with income levels, but with diminishing marginal pollution at higher income levels.

To assess the relationship between income levels and air pollution from coal plants, we conduct a global analysis at the country level. We aggregate pixel-level data on SO_2 pollution and the Human Development Index (HDI) up to the country level. For SO_2, we use the pollution maps produced for this study (see Section); for HDI and GDP, we use Kummu et al. (2018); for population, data is obtained from CIESIN (2016) to compute national GDP per capita. The number of power plants in a given country is based on Shearer et al. (2021) (see Section 3.1).

We find a positive and strong correlation between the number of coal power plants and national income levels (Figure 9); i.e. countries with higher incomes tend to have more coal

power plants. The upper three figures are for all countries other than the top four countries with more than 200 power plants

Figure 9: Global analysis at the country level: #plants and income

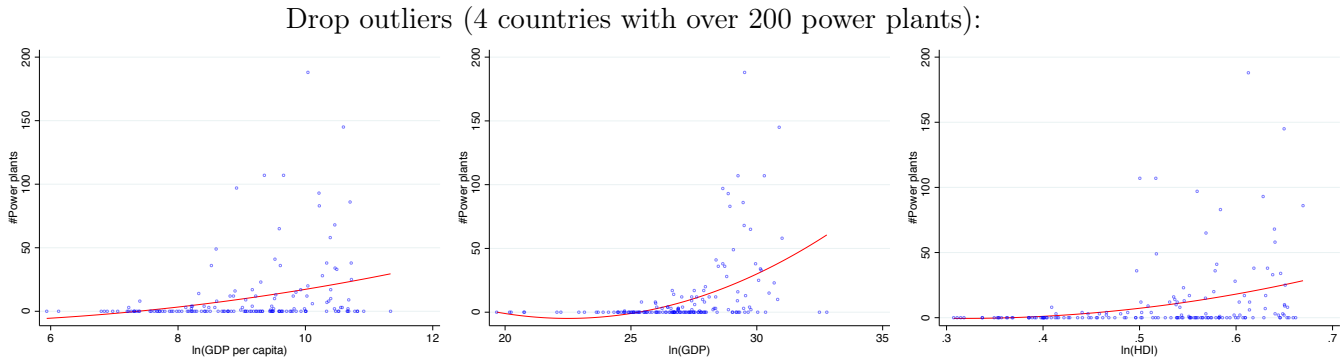

When considering the relationship between national average SO_2 concentrations and incomes, we find similar patterns that are consistent with the number of coal plants (Figure 10); i.e. countries with higher incomes tend to face more pollution from coal power plants. The correlation is positive and concave, suggesting that the increase in SO_2 levels is slower at higher levels of GDP per capita. This finding is consistent with the notion that countries at higher income levels may move away from polluting energy sources, such as coal, and transition to cleaner, more efficient alternatives. National GDP also shows a positive but convex relationship with SO_2, suggesting that higher GDP levels are associated with increasingly higher SO_2 pollution. Our interpretation is that GDP measures economic output, while GDP per capita measures wealth or income. Economic outputs are mechanically always correlated with GDP, but income may show an increasing then decreasing pattern if rich people move to clean areas. We see similar estimates in tabular results in Table 3. GDP per capita is positively correlated with SO_2, but the quadratic fit shows an increasing and then decreasing pattern.

Besides these country-level results, we also assess the relationship between income levels and pollution exposure by conducting a pixel-level analysis. Gridded GDP, GDP per capita, and SO_2 data enable us to consider a sample of over 11 million unique locations (i.e. pixels). This enables us to capture granular sub-national variations, thus distinguishing between areas with different pollution and income levels with high precision of estimation. The results, summarized in Table 4, are consistent with the findings of the country-level analysis. Across the world, higher-income areas tend to be exposed to higher SO_2 pollution from coal-fired power plants. Every additional 10% increase in GDP per capita is associated with 1.64% higher SO_2 pollution.

We use additional flexible fittings to explore the potential nonlinear relationship between air

Figure 10: Global analysis at the country level: pollution and income

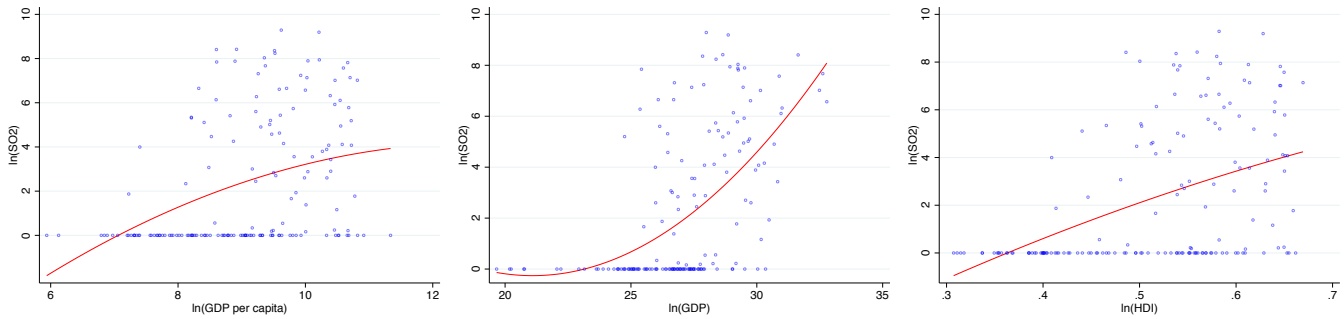

pollution and income levels. First, we use restricted cubic splines with 10 knots, which yields results (summarized in Figure 12) consistent with country-level results in Figure 10. GDP per capita and pollution display a concave relationship, while GDP has a convex relationship with pollution. Other flexible fitting methods, including a non-parametric kernel regression (Figure 13) and a binning regression (Figure 14) based on (Schlenker and Roberts, 2009), confirm the findings from the polynomial fits in the country- and pixel-level analyses.

In addition, we conduct several sensitivity checks in Section S2.3. First, over half of the considered countries have no coal-fired power plant, so their modeled SO_2 concentrations are low (residual SO_2 concentrations are due to transboundary pollution). We test the robustness of the above findings by restricting the sample to (i) 71 countries that have at least one power plant; (ii) countries with a higher number of power plants than the median; and (iii) countries with a plant count in the top quartile. The refined sample sizes are smaller, but the average SO_2 and the 90 percentile of SO_2 in the remaining countries are larger. Average SO_2 measures the ambient air quality of a representative person in that country, while the 90 percentile captures pollution faced by the group with the least favorable air quality. Higher values suggest countries with more power plants are generally more polluting. Results are reported in Section S2.3, and are consistent with the main findings from the pixel-level analysis presented in Table 4.

Moreover, we conduct an additional analysis in which we only consider pixels within a 2-degree radius of coal plants to study local inequality in exposure. This controls for the pattern that power plants tend to be built in more industrialized and economically active areas. Even in this restricted sample, higher GDP per capita levels are associated with higher pollution levels, with diminishing marginal pollution for high income levels. GDP also displays a positive and convex relationship with pollution, thus supporting the robustness of our findings. In the case of HDI, areas with medium-level HDI scores tend to face the highest pollution exposure compared

with those whose HDI scores are higher or lower. We interpret results on HDI variation with caution, as the gridded HDI data by Kummu et al. (2018) display very limited subnational variation.

4.3 'Strategic' location choice

In this section, we explore the notion that location choices for polluting power plants are not made at random. Case study evidence, especially from the U.S., documents that low-income and ethnic minority communities are disproportionately exposed to air pollution. We analyze the relationship between income and air pollution for over 1.3 million unique locations (pixels) around over 3,800 coal plants. We find that power plant locations are indeed not evenly distributed across income groups. In the proximity of coal plants, downwind areas are systematically poorer than upwind areas. Poorer communities are disproportionately exposed to toxic pollution from coal plants.

This pattern could be explained by several factors: When deciding plant locations, operators may strategically select spots where prevailing wind directions mean that pollutants are carried to lower-income communities. These communities are likely to have lower bargaining power to oppose such siting decisions. This regressive environmental burden may be further aggravated by spatial sorting once the plant assumes operations. As environmental quality (including air quality) is priced into land values, high-income households are able to sort into cleaner upwind areas, while low-income households are more likely to move into cheaper, more polluted areas.

To assess systematic inequalities in pollution exposure, we conduct a single difference analysis designed to test if plants' downwind directions are associated with lower income levels. We estimate the following model:

$$Y_{ij} = \beta Downwind_{ij} + Plant_i + \varepsilon_{ij} \tag{1}$$

where the sample is at the plant-pixel level. We use the year when plants started to operate to code dependent variables, where start years differ across plants. In the first stage, we use SO_2 at recipient pixel j near plant i. Our sample consists of pixels that are located within a 0.5-degree radius around plants, and located in up- or downwind locations. Pixels in crosswind directions are dropped. If the prevailing wind direction at a plant has a reference angle of 0°, upwind pixels are defined as those located within -45° to 45° around plants, while downwind areas are located within 135° to 180° and -180° to -135°.

$Downwind_{ij}$ is a binary variable that is one if pixel j is in the downwind direction of plant

i and zero if it is in the upwind direction. We add plant fixed effects as control variables to capture all covariates in each plant's surrounding areas. We expect β_1 to be positive when using SO_2 as the outcome variable. It measures the pollution difference in downwind areas compared with upwind areas. In the reduced form analysis, we use GDP, GDP per capita, and HDI as dependent variables. Our hypothesis holds if the estimated β_1 is negative, which suggests that downwind pixels tend to be poorer than upwind pixels.

Results, summarized in Table 1, show that downwind areas are indeed associated with higher air pollution, as well as lower income. Specifically, downwind areas witness 13 percent higher SO_2 concentrations, 2.9 percent lower GDP per capita, and 0.2 percent lower HDI value. The lower panel reports results after controlling for plant fixed effects. R^2 increases to 0.3 when SO_2 is on the left-hand side, and increases to over 0.9 with economic outputs as dependent variables. Compared with upwind pixels near the same plant, downwind regions still have 13 percent more air pollution, 1.6 percent lower GDP per capita, 2.5 percent lower GDP, and 0.1 percent lower HDI. The differences are equivalent to 0.17, 0.19, and 0.01 standard deviations in GDP per capita, GDP, and HDI respectively. These estimates confirm the hypothesis that more polluted downwind areas tend to host lower-income communities. Findings are consistent with the notion that plant location choices are influenced by the income profile of surrounding areas, and that air pollution may reinforce the low-income status of downwind areas through spatial sorting effects.

As a robustness check, we use an alternative angle to define upwind and downwind areas. Instead of 90°, we use a narrower angle of 60° to define upwind and downwind areas. Results for this specification, summarized in Section S2.1, are consistent with the main results presented above. We also use alternative distance thresholds to define pollution-affected areas. Instead of a 0.5-degree radius around plants, we restrict the sample to pixels within a 0.3 degree (roughly 35km) radius and re-estimate the model. These results are also consistent with the main findings (Section S2.1).

Compared with results in Table 1, Table 2 shows a larger difference between downwind and upwind pollution. The single difference analysis adopts cross-sectional data at the plant level and only uses the year when the operation started, while the double-difference analysis uses panel data for all years 1992-2013. This suggests plant operation exacerbates the inequality between pollution exposure.

4.4 Does air pollution cause a reduction in income levels?

Air pollution has been documented to be detrimental to health and productivity, and thus indirectly people's incomes. In this section, we use a difference-in-difference design to test the potential impact of air pollution on income levels. We compare pollution levels and economic indicators in downwind and upwind areas, before and after the activation of new coal plants. First stage results confirm that differences in pollution levels are insignificant before activation, but post-activation pollution levels are significantly higher in downwind areas. However, reduced form results do not confirm meaningful differences between the income levels in up- and downwind locations. Thus, these results do not yield robust evidence that air pollution causes reductions in income levels. This result is documented in this section for the sake of completeness, and to inform future efforts for a causal identification with global coverage. Possible factors that can explain this null result are the relatively short time series of data (which may not allow long-term health and productivity effects to materialize), and the fact that health-related expenditures are included in indicators of economic activity thus diluting the impact.

To evaluate the causal effect of power plants' operation on local economic indicators, we use a difference-in-difference design that compares upwind and downwind pixels before and after coal plant activation. The econometric specifications are as follows:

$$\begin{aligned} Y_{ijt} = \beta_1 Downwind_{ij} + \beta_2 Operating_{jt} \\ + \beta_3 Downwind_{ij} \times Operating_{jt} \\ + Pixel_i + Year_t + \varepsilon_{ijt} \end{aligned} \tag{2}$$

where the sample is at the year-plant-pixel level. The time range is the same as the gridded income dataset, i.e. 1990-2015. To ensure that pre- and post-activation periods are included, we restrict the sample consists to 2,380 coal power units that were activated between 1992-2013 (i.e. disregarding 3,941 units that were activated outside this time frame or have missing commission years). Besides, we include up- and downwind pixels that are located within a 0.5-degree radius around plants, and drop those in crosswind directions. Upwind pixels are defined as those located -45° to 45° around plants, while downwind areas are located 135° to 180° and -180° to -135°. Upwind and downwind areas are visualized in Figure 3.

The dependent variable Y_{ijt} in the first stage is SO_2 in recipient pixel i near plant j in year t. In the reduced form, Y_{ijt} is pixel-level GDP, GDP per capita, or HDI. On the right-hand side, $Downwind_{ij}$ is a dummy that is one if pixel i is in the downwind direction of plant j and zero otherwise. $Operating_{jt}$ is an indicator that equals one if plant j started to operate in or

before year t and zero otherwise. Standard errors are clustered at the plant level to capture the autocorrelation within a given plant location across nearby pixels across time. Coefficient β_2 captures the impact of plant operation on upwind pollution and income. Coefficient $\beta_2 + \beta_3$ measures the impact of operations on downwind pollution and income. Note that β_1 is not absorbed by $Pixel_i$ as pixels could be in the upwind direction of some plants but in the downwind direction of others.

Figure 11 offers a visual summary of the diff-in-diff analysis. The horizontal axis denotes the year relative to the operation start year. Red lines represent downwind pixels, while blue lines depict upwind pixels. The first stage analysis (Figure 11 left) highlights a stark increase in the pollution levels of downwind locations. Upwind areas observe a slight increase due to upwind pollution in the immediate vicinity of plants. The same pattern is not apparent in the reduced form (Figure 11 right); GDP per capita at the pixel level does not display significant differences between up- and downwind locations following the activation of coal plants. For related charts on GDP and HDI, refer to Figure S4.2.

Figure 11: Event study figures

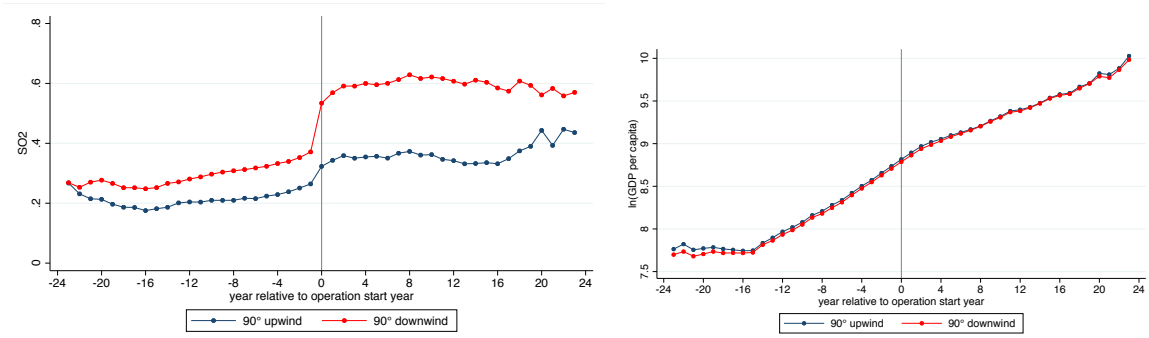

Notes: Y-axis in the left panel is in the logged unit. Average SO_2 among all pixels that are upwind before operations is 0.214 in the figure logged unit, 0.815 in $\mu g/m^3$; That for downwind pre-period is 0.291 in the figure logged unit, 1.20 in $\mu g/m^3$; upwind after: 0.365 and 1.53$\mu g/m^3$; downwind after: 0.593 and 2.46$\mu g/m^3$.

Full first stage and reduced form results are reported in Table 2 and Table S3.1, respectively. After plant operations, downwind regions have 17.7 percent higher SO_2 compared with the same pixel before operations. In contrast, upwind regions only have a 3 percent increase in SO_2. This indicates a strong first stage result - plant operations significantly worsen air quality in downwind areas; upwind areas serve as counterfactuals. However, reduced form results report small and insignificant estimates, suggesting that upwind and downwind areas behave similarly in their income levels. In short, these results can neither support nor refute the notion that coal-plant driven air pollution causes income reductions in affected areas.

For completeness, we check for potential heterogeneous responses with respect to the start year of coal plants, as well as national pollution and income levels. The hypothesis is that countries with lower incomes and higher pollution levels may prioritize economic growth, and thus respond differently than high-income low-pollution countries. However, results reported in Table S3.2, S3.3 and S3.4 still show small and imprecise estimates on the interaction term with economic variables as left-hand sides, indicating negligible impacts of plant operations on income levels regardless of countries' development stages. Section S2.2 summarizes findings from a set of sensitivity checks. Results remain strongly robust to alternative definitions of up- and downwind areas to construct the sample (i.e. alternative angles and distances).

There are at least three potential reasons for the null results in this section. First, adverse impacts of pollution on health and labor productivity may take many years to materialize. The time ranges considered in our sample may not be long enough to capture a meaningful reduction in income levels. Second, the GDP and HDI data are constructed using national economic values and subnational population as inputs (Kummu et al., 2018). Compared with our detailed pollution trajectory modeling, income data may not be granular enough to capture small-scaled local differences. Third, even if air pollution affects health outcomes and the quality of life, this may not translate into a significant reduction in income levels. On the contrary, high spending on healthcare could even push up measures of national production, such as GDP.

5 Conclusion

Many countries continue to rely on coal power plants for electricity generation, despite their tremendous financial, societal, and environmental costs. This paper documents inequalities in people's exposure to toxic air pollutant emissions from the world's almost 4,000 coal-fired power plants. By modeling the wind-dispersion of air pollutants, we generate a high-resolution wind-directed global air pollution map for coal plants. We find that, globally, 2.32 billion people are exposed to air pollution originating from coal power plants. Globally, 160 million people face SO_2 pollution from coal plants that exceed the World Health Organization (WHO) guideline value of 40 $\mu g/m^3$ – and this does not account for pollution from other sources. Moreover, 247.5 million people are exposed to transboundary pollution – namely, toxic air pollution originating from coal plants outside their country.

We find that, overall, air pollution from coal plants increases with income levels. Richer areas have more coal plants, thus more coal plant-related pollution. However, air pollution from coal plants increases at a diminishing rate at high income levels. This is consistent with the notion that high-income countries transition to more efficient less polluting power sources. Our results

are consistent for different country samples, at subnational levels, and multiple non-parametric fitting.

We also evaluate the local-scale pollution inequality in the proximity of coal plants. We find that areas located downwind from coal plants are systematically associated with higher pollution and lower income levels compared to areas upwind. This is indicative of two distinct mechanisms that are likely to be at play: The initial siting choices for coal-fired power plants are influenced by the socioeconomic context of sites. Plant locations are systematically chosen in a way that the air pollution burden of plants falls disproportionately on lower-income communities. Moreover, once sites are operational, air pollution levels are reflected in property values and influence spatial sorting decisions of communities. High pollution levels could then reinforce the low-income status of affected communities.

Overall, this work contributes to the simulation methods of pollutant trajectory. We combine HYSPLIT and Gaussian dispersion to track the three-dimensional pathways of air masses. This enables the first large-scale assessment of pollution exposure inequality associated with coal-fired power plants. Future research could further disentangle the mechanisms that drive unequal pollution exposure, and explore the causal effect of plant operation on poverty and income levels – for instance, using longer time series to take into account the long-term impacts of pollution on lives and livelihoods.

Table 1: Single difference results

	$\ln(SO_2)$	ln(GDP per capita)	ln(GDP)	ln(HDI)
	(1)	(2)	(3)	(4)
Downwind	0.132***	-0.029**	-0.022	-0.002**
	(0.010)	(0.013)	(0.016)	(0.001)
ln(Population)			0.972***	
			(0.014)	
Observations	1345071	1345071	1345071	1345071
R-square	0.031	0.000	0.809	0.000
Downwind	0.132***	-0.016**	-0.025*	-0.001*
	(0.010)	(0.007)	(0.013)	(0.001)
ln(Population)			1.163***	
			(0.017)	
Observations	1345071	1345071	1345071	1345071
R-square	0.333	0.965	0.946	0.965
Y-mean	0.271	8.801	17.786	0.511
Y-sd	0.377	0.835	2.287	0.061
Plant FEs	Y	Y	Y	Y

Notes: Standard errors are clustered at the plant level.

Table 2: First stage results

	$\ln(SO_2)$			
	(1)	(2)	(3)	(4)
Operating	0.138***	0.169***	0.016	0.030***
	(0.016)	(0.008)	(0.025)	(0.007)
Downwind	0.087***	-0.058***	0.087***	-0.057***
	(0.017)	(0.005)	(0.017)	(0.004)
Operating × Downwind	0.152***	0.148***	0.151***	0.147***
	(0.019)	(0.011)	(0.019)	(0.011)
Observations	34971846	34971846	34971846	34971846
R-square	0.038	0.871	0.047	0.878
Y-mean	0.347	0.347	0.347	0.347
Y-sd	0.691	0.691	0.691	0.691
Pixel FEs		Y		Y
Year FEs			Y	Y

Notes: Standard errors are clustered at the plant level.

Table 3: Global analysis at the country level

	Panel A: ln(SO_2) and ln(GDP per capita)		
	(1)	(2)	(3)
ln(GDP per capita)	1.002***	3.319	-41.365*
	(0.188)	(2.606)	(22.904)
ln(GDP per capita)^2		-0.130	5.054*
		(0.146)	(2.644)
ln(GDP per capita)^3			-0.198*
			(0.101)
Observations	166	166	166
R-square	0.147	0.152	0.171
Y-mean	2.289	2.289	2.289
Y-sd	2.947	2.947	2.947
	Panel B: ln(SO_2) and ln(GDP)		
ln(GDP)	0.931***	-2.084*	-6.628
	(0.160)	(1.174)	(12.545)
ln(GDP)^2		0.056**	0.230
		(0.021)	(0.479)
ln(GDP)^3			-0.002
			(0.006)
ln(Population)	-0.348*	-0.270	-0.252
	(0.180)	(0.180)	(0.187)
R-square	0.298	0.326	0.326
	Panel C: ln(SO_2) and ln(HDI)		
ln(HDI)	14.144***	23.110	-156.958
	(2.159)	(23.560)	(176.894)
ln(HDI)^2		-8.978	361.847
		(23.493)	(361.809)
ln(HDI)^3			-248.442
			(241.890)
Observations	166	166	166
R-square	0.207	0.208	0.213
Y-mean	2.289	2.289	2.289
Y-sd	2.947	2.947	2.947

Notes: ln(GDP per capita)^2 is the square of log of GDP per capita. Unit of SO_2: nano gram/m^3, unit of GDP and GDP per capita: constant 2011 international US dollar.

Table 4: Global analysis at the pixel level

	Panel A: ln(SO_2) and ln(GDP per capita)			
	(1)	(2)	(3)	(4)
ln(GDP per capita)	0.190***	0.618	-6.126**	-7.206**
	(0.066)	(0.791)	(3.007)	(2.969)
ln(GDP per capita)^2		-0.024	0.735**	0.823**
		(0.046)	(0.342)	(0.330)
ln(GDP per capita)^3			-0.028**	-0.030**
			(0.013)	(0.012)
Observations	11163331	11163331	11163331	11163331
R-square	0.016	0.017	0.020	0.145
Y-mean	0.493	0.493	0.493	0.493
Y-sd	1.790	1.790	1.790	1.790
	Panel B: ln(SO_2) and ln(GDP)			
ln(GDP)	0.164***	-0.731***	0.106	0.380
	(0.040)	(0.174)	(0.454)	(0.338)
ln(GDP)^2		0.030***	-0.027	-0.043*
		(0.007)	(0.035)	(0.026)
ln(GDP)^3			0.001	0.001**
			(0.001)	(0.001)
ln(Population)	0.048	0.012	0.015	0.111***
	(0.042)	(0.036)	(0.037)	(0.029)
R-square	0.083	0.108	0.109	0.197
	Panel C: ln(SO_2) and ln(HDI)			
ln(HDI)	2.786***	-1.213	9.022	-102.199
	(0.753)	(9.863)	(50.113)	(63.811)
ln(HDI)^2		3.987	-16.853	211.375
		(9.928)	(109.894)	(129.588)
ln(HDI)^3			13.788	-138.517
			(77.635)	(83.864)
R-square	0.020	0.021	0.021	0.147
Country FEs				Y

Notes: Unit of SO_2: nano gram/m^3, unit of GDP and GDP per capita: constant 2011 international US dollar. Standard errors are clustered at the country level.

Figure 12: Restricted cubic splines

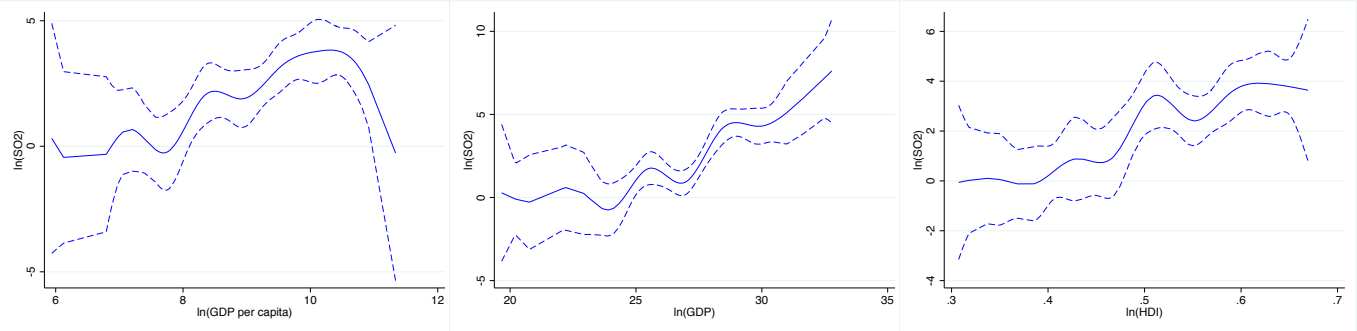

Figure 13: Nonparametric kernel fitting

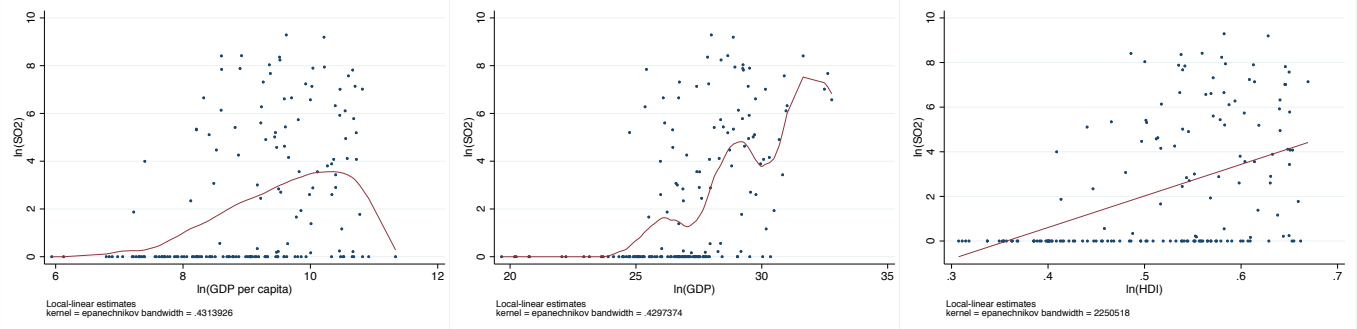

Figure 14: Eighth-order polynomial for each income bin

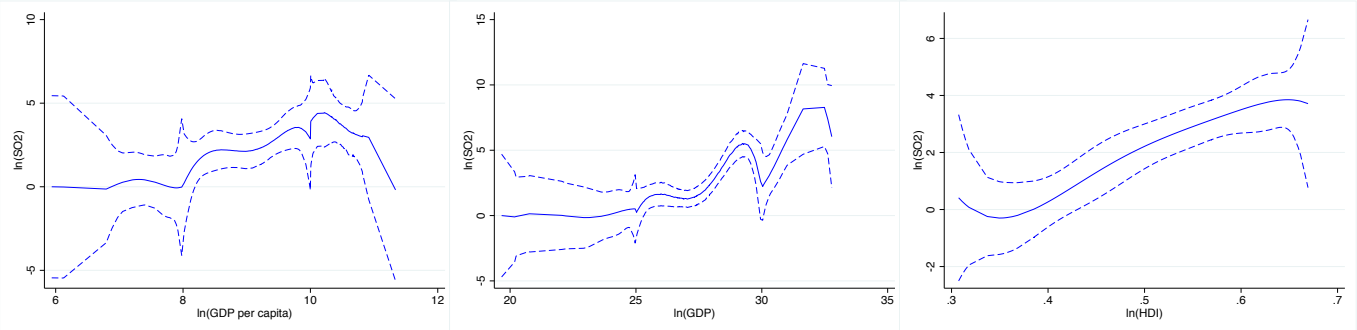

References

Agency, U. E. P. (1995). A user's guide for the calpuff dispersion model. *Research Triangle Park, N.C.*.

Anderson, M. L. (2019, 10). As the Wind Blows: The Effects of Long-Term Exposure to Air Pollution on Mortality. *Journal of the European Economic Association 18*(4), 1886–1927.

Arceo, E., R. Hanna, and P. Oliva (2016). Does the effect of pollution on infant mortality differ between developing and developed countries? evidence from mexico city. *The Economic Journal 126*(591), 257–280.

Arora, S. and T. N. Cason (1999). Do community characteristics influence environmental outcomes? evidence from the toxics release inventory. *Southern Economic Journal 65*(4), 691–716.

Barrows, G., T. Garg, and A. Jha (2019, December). The health costs of coal-fired power plants in india. *IZA Discussion Paper Series* (12838).

Barwick, P. J., S. Li, D. Rao, and N. B. Zahur (2018, June). The healthcare cost of air pollution: Evidence from the world's largest payment network. Working Paper 24688, National Bureau of Economic Research.

Been, V. and F. Gupta (1997). Coming to the nuisance or going to the barrios? a longitudinal analysis of environmental justice claims. *Ecology Law Quarterly 24*(1), 1–56.

Boer, J. T., M. Pastor, J. L. Sadd, and L. D. Snyder (1997). Is there environmental racism? the demographics of hazardous waste in los angeles county. *Social Science Quarterly 78*(4), 793–810.

Burnett, R., H. Chen, M. Szyszkowicz, N. Fann, B. Hubbell, C. A. Pope, J. S. Apte, M. Brauer, A. Cohen, S. Weichenthal, J. Coggins, Q. Di, B. Brunekreef, J. Frostad, S. S. Lim, H. Kan, K. D. Walker, G. D. Thurston, R. B. Hayes, C. C. Lim, M. C. Turner, M. Jerrett, D. Krewski, S. M. Gapstur, W. R. Diver, B. Ostro, D. Goldberg, D. L. Crouse, R. V. Martin, P. Peters, L. Pinault, M. Tjepkema, A. van Donkelaar, P. J. Villeneuve, A. B. Miller, P. Yin, M. Zhou, L. Wang, N. A. H. Janssen, M. Marra, R. W. Atkinson, H. Tsang, T. Q. Thach, J. B. Cannon, R. T. Allen, J. E. Hart, F. Laden, G. Cesaroni, F. Forastiere, G. Weinmayr, A. Jaensch, G. Nagel, H. Concin, and J. V. Spadaro (2018). Global estimates of mortality associated with long-term exposure to outdoor fine particulate matter. *Proceedings of the National Academy of Sciences 115*(38), 9592–9597.

Carpenter, A. and M. Wagner (2019). Environmental justice in the oil refinery industry: A panel analysis across united states counties. *Ecological Economics 159*, 101–109.

Chang, T. Y., J. Graff Zivin, T. Gross, and M. Neidell (2019, January). The effect of pollution on worker productivity: Evidence from call center workers in china. *American Economic Journal: Applied Economics 11*(1), 151–72.

Chen, S., P. Oliva, and P. Zhang (2022). The effect of air pollution on migration: Evidence from china. *Journal of Development Economics 156*, 102833.

Chen, S. and D. Zhang (2021). Impact of air pollution on labor productivity: Evidence from prison factory data. *China Economic Quarterly International 1*(2), 148–159.

CIESIN (2016). Gridded population of the world, version 4 (gpwv4): Administrative unit center points with population estimates.

Cropper, M., R. Cui, S. Guttikunda, N. Hultman, P. Jawahar, Y. Park, X. Yao, and X.-P. Song (2021). The mortality impacts of current and planned coal-fired power plants in india. *Proceedings of the National Academy of Sciences 118*(5), e2017936118.

Deryugina, T., G. Heutel, N. H. Miller, D. Molitor, and J. Reif (2019, December). The mortality and medical costs of air pollution: Evidence from changes in wind direction. *American Economic Review 109*(12), 4178–4219.

Deschenes, O., M. Greenstone, and J. S. Shapiro (2017, October). Defensive investments and the demand for air quality: Evidence from the nox budget program. *American Economic Review 107*(10), 2958–89.

Du, X., X. Jin, N. Zucker, R. Kennedy, and J. Urpelainen (2020). Transboundary air pollution from coal-fired power generation. *Journal of Environmental Management 270*, 110862.

EPA (2020). Environmental justice. https://www.epa.gov/environmentaljustice/learn-about-environmental-justice. Accessed: 2022-05-05.

Fan, M., G. He, and M. Zhou (2020). The winter choke: Coal-fired heating, air pollution, and mortality in china. *Journal of Health Economics 71*, 102316.

Gennaioli, N., R. La Porta, F. Lopez-de Silanes, and A. Shleifer (2012, 11). Human Capital and Regional Development *. *The Quarterly Journal of Economics 128*(1), 105–164.

Graff Zivin, J. and M. Neidell (2012, December). The impact of pollution on worker productivity. *American Economic Review 102*(7), 3652–73.

Graham, J. D., N. D. Beaulieu, D. Sussman, M. Sadowitz, and Y.-C. Li (1999). Who lives near coke plants and oil refineries? an exploration of the environmental inequity hypothesis. *Risk Analysis 19*(2), 171–186.

Gray, M., S. Ljungwaldh, L. Watson, and I. Kok (2018, 11). Powering down coal: Navigating the economic and financial risks in the last years of coal power. *The Carbon Tracker Initiative*.

Greenstone, M. and R. Hanna (2014, October). Environmental regulations, air and water pollution, and infant mortality in india. *American Economic Review 104*(10), 3038–72.

Hanlon, W. W. (2019, 10). Coal Smoke, City Growth, and the Costs of the Industrial Revolution. *The Economic Journal 130*(626), 462–488.

He, G., M. Fan, and M. Zhou (2016). The effect of air pollution on mortality in china: Evidence from the 2008 beijing olympic games. *Journal of Environmental Economics and Management 79*, 18–39.

He, J., H. Liu, and A. Salvo (2019, January). Severe air pollution and labor productivity: Evidence from industrial towns in china. *American Economic Journal: Applied Economics 11*(1), 173–201.

Heblich, S., A. Trew, and Y. Zylberberg (2021). East-side story: Historical pollution and persistent neighborhood sorting. *Journal of Political Economy 129*(5), 1508–1552.

HEI (2020). State of global air 2020.

Helland, E. and A. B. Whitford (2003). Pollution incidence and political jurisdiction: evidence from the tri. *Journal of Environmental Economics and Management 46*(3), 403–424.

Imelda (2018, May). Indoor air pollution and infant mortality: A new approach. *AEA Papers and Proceedings 108*, 416–21.

Ito, K. and S. Zhang (2020). Willingness to pay for clean air: Evidence from air purifier markets in china. *Journal of Political Economy 128*(5), 1627–1672.

Khanna, G., W. Liang, A. M. Mobarak, and R. Song (2021, January). The productivity consequences of pollution-induced migration in china. Working Paper 28401, National Bureau of Economic Research.

Kleist, D. T., D. F. Parrish, J. Derber, R. E. Treadon, W. Wu, and S. J. Lord (2009). Introduction of the gsi into the ncep global data assimilation system. *Weather and Forecasting 24*, 1691–1705.

Kummu, M., M. Taka, and J. Guillaume (2018, 02). Gridded global datasets for gross domestic product and human development index over 1990–2015. *Scientific Data 5*, 180004.

Kushta, J., N. Paisi, H. D. V. D. Gon, and J. Lelieveld (2021, mar). Disease burden and excess mortality from coal-fired power plant emissions in europe. *Environmental Research Letters 16*(4), 045010.

Li, C., N. A. Krotkov, P. J. T. Leonard, S. Carn, J. Joiner, R. J. D. Spurr, and A. Vasilkov (2020). Version 2 ozone monitoring instrument so_2 product (omso2 v2): new anthropogenic so_2 vertical column density dataset. *Atmospheric Measurement Techniques 13*(11), 6175–6191.

Lipscomb, M. and A. M. Mobarak (2016, 11). Decentralization and Pollution Spillovers: Evidence from the Re-drawing of County Borders in Brazil*. *The Review of Economic Studies 84*(1), 464–502.

Liu, F., Q. Zhang, D. Tong, B. Zheng, M. Li, H. Huo, and K. B. He (2015). High-resolution inventory of technologies, activities, and emissions of coal-fired power plants in china from 1990 to 2010. *Atmospheric Chemistry and Physics 15*(23), 13299–13317.

Lu, Z. and D. Streets (2012, 06). Increase in nox emissions from indian thermal power plants during 1996-2010: Unit-based inventories and multisatellite observations. *Environmental science & technology 46*, 7463–70.

Lueken, R., K. Klima, W. M. Griffin, and J. Apt (2016). The climate and health effects of a usa switch from coal to gas electricity generation. *Energy 109*, 1160–1166.

Manisalidis, I., E. Stavropoulou, A. Stavropoulos, and E. Bezirtzoglou (2020, 02). Environmental and health impacts of air pollution: A review. *Frontiers in Public Health 8*.

Marais, E., R. Silvern, A. Vodonos, E. Dupin, A. Bockarie, L. Mickley, and J. Schwartz (2019, 10). Air quality and health impact of future fossil fuel use for electricity generation and transport in africa. *Environmental Science Technology 2019*.

Miller, C. (1978). An examination of gaussian plume dispersion parameters for rough terrain. *Atmospheric Environment (1967) 12*(6), 1359–1364.

Monogan III, J. E., D. M. Konisky, and N. D. Woods (2017). Gone with the wind: Federalism and the strategic location of air polluters. *American Journal of Political Science 61*(2), 257–270.

Morehouse, J. and E. Rubin (2021, 4). Downwind and Out: The Strategic Dispersion of Power Plants and their Pollution. *Available at SSRN*.

Orellano, P., J. Reynoso, and N. Quaranta (2021). Short-term exposure to sulphur dioxide (so2) and all-cause and respiratory mortality: A systematic review and meta-analysis. *Environment International 150*, 106434.

Parry, I., S. Black, and N. Vernon (2021, 9). Still not getting energy prices right: A global and country update of fossil fuel subsidies. *International Monetary Fund Working Paper* (236).

Penney, S., J. Bell, and J. Balbus (2009, 01). Estimating the health impacts of coal-fired power plants receiving international financing.

Rentschler, J. and N. Leonova (2022). Air pollution and poverty : Pm2.5 exposure in 211 countries and territories. *World Bank Policy Research Working Paper*.

Schlenker, W. and M. J. Roberts (2009). Nonlinear temperature effects indicate severe damages to u.s. crop yields under climate change. *Proceedings of the National Academy of Sciences 106*(37), 15594–15598.

Schlenker, W. and W. R. Walker (2015, 10). Airports, Air Pollution, and Contemporaneous Health. *The Review of Economic Studies 83*(2), 768–809.

Shearer, C., N. Ghio, L. Myllyvirta, A. Yu, and T. Nace (2021). Boom and bust 2021: Tracking the global coal plant pipeline. *Global Energy Monitor*.

Sigman, H. (2005). Transboundary spillovers and decentralization of environmental policies. *Journal of Environmental Economics and Management 50*(1), 82–101.

Tong, D., Q. Zhang, S. Davis, F. Liu, B. Zheng, G. Geng, T. Xue, M. Li, C. Hong, Z. Lu, D. Streets, D. Guan, and H. He (2018, 01). Targeted emission reductions from global super-polluting power plant units. *Nature Sustainability 1*.

van Donkelaar, A., M. S. Hammer, L. Bindle, M. Brauer, J. R. Brook, M. J. Garay, N. C. Hsu, O. V. Kalashnikova, R. A. Kahn, C. Lee, R. C. Levy, A. Lyapustin, A. M. Sayer, and R. V. Martin (2021). Monthly global estimates of fine particulate matter and their uncertainty. *Environmental Science & Technology 55*(22), 15287–15300. PMID: 34724610.

Vohra, K., A. Vodonos, J. Schwartz, E. A. Marais, M. P. Sulprizio, and L. J. Mickley (2021). Global mortality from outdoor fine particle pollution generated by fossil fuel combustion: Results from geos-chem. *Environmental Research 195*, 110754.

Wolverton, A. (2009). Effects of socio-economic and input-related factors on polluting plants' location decisions. *The B.E. Journal of Economic Analysis & Policy 9*(1).

Zhang, J. and Q. Mu (2018). Air pollution and defensive expenditures: Evidence from particulate-filtering facemasks. *Journal of Environmental Economics and Management 92*, 517–536.

Zhong, N., J. Cao, and Y. Wang (2017). Traffic congestion, ambient air pollution, and health: Evidence from driving restrictions in beijing. *Journal of the Association of Environmental and Resource Economists 4*(3), 821 – 856.

Zwickl, K., M. Ash, and J. K. Boyce (2014). Regional variation in environmental inequality: Industrial air toxics exposure in u.s. cities. *Ecological Economics 107*, 494–509.

Online Appendix

S1 Health effects

By comparing modeled pollution levels from this study with overall pollution levels, we estimate the marginal health impacts associated with pollution from coal plants. For this purpose, we first estimate what total pollution levels would be in the absence of coal plants.

In the case of SO_2 pollution, the marginal contribution of coal plants is calculated as: *coal-free* SO_2 = *total* SO_2 − *modeled* SO_2 contribution from coal plants. Baseline *total* SO_2 levels are obtained from the NASA Ozone Monitoring Instrument (OMI) (Li et al., 2020). It measures the daily mean SO_2 concentration for each 0.25-degree pixel with global coverage. We compute the average annual SO_2 concentration for 2013 and replicate the same value for all 0.01-degree pixels. We then subtract the marginal contribution from coal plants.

We follow a similar procedure for the case of $PM_{2.5}$. The marginal contribution of coal plants is calculated as: *coal-free* $PM_{2.5}$ = *total* $PM_{2.5}$ − *modeled* $PM_{2.5}$ contribution from coal plants. Baseline *total* $PM_{2.5}$ in 2013 is obtained from van Donkelaar et al. (2021), who provide a monthly product with a spatial resolution of 0.01 degrees. $PM_{2.5}$ contributions from coal-fired power plants are simulated using similar methods as for SO_2 (see Section 4.2). While we are not able to track the emission of primary $PM_{2.5}$ or secondary $PM_{2.5}$ formed from chemical conversions, we also simulate particle emissions based on emission inventory data described in Section 3.1.

The next step is to estimate air pollution deaths associated with the marginal contribution of coal-fired power plants. We follow Cropper et al. (2021) to calculate baseline deaths due to air pollution from power plants:

$$\sum_i M_i = \lambda_i \times RR(Pollution_i) \times Population_i$$

where M_i represents deaths in pixel i. λ_i denotes the death rate at the background level. While λ_i is not observable, we estimate λ_i using mortality caused by baseline air pollution, 4.5 million per year documented by HEI (2020). $RR(Pollution_i)$ is the relative risk of death at the exposure level. $Population_i$ is the population size at the grid cell level. Air pollution deaths without the contribution of coal plants ($\sum_i \Delta M_i$) can then be estimated as:

$$\sum_i \Delta M_i = \lambda_i \times RR(Pollution_i - CoalPollution_i) \times Population_i$$

where $CoalPollution_i$ is the simulated plants' contribution in pixel i's air pollution.

We separately estimate effects of SO_2 and $PM_{2.5}$ using dose-response functions from Orellano et al. (2021) and Burnett et al. (2018). $PM_{2.5}$ has a concave relationship with mortality risk, with hazardous ratios ranging from 1 to 1.8 (Burnett et al., 2018). Regarding SO_2, Orellano et al. (2021) conduct a meta-analysis to aggregate individual results on SO_2 and death risks. An increase of 10 $\mu g/m^3$ in the 24-hour average exposure to SO_2 is associated with an increase in all-cause mortality, with relative risk estimated as 1.0059. Therefore, we use a linear relative risk function by $PM_{2.5}$ levels and constant relative risk for SO_2 estimates.

Our modeled results suggest that 1.4 million deaths are caused by SO_2 emitted from coal-fired power plants. Among them, 0.24 million deaths and 0.61 million deaths are from India and China respectively. For $PM_{2.5}$, 2.4 million deaths are associated with pollution from coal-fired power plants. China and India take account of 1.44 million and 0.55 million deaths, 59.8% and 22.9% of the global total. It should be noted that air pollution refers to the accumulation of many different types of pollutants. Thus, we do not attempt to add these two values since the effects are not mutually exclusive. Instead, we consider 2.4 million deaths to be the lower bound estimate for deaths associated with coal power plants.

Table S1.1: Exposed population and deaths due to coal plant pollution in top 5 countries

	Total population exposed to coal plant pollution (millions)	Annual air pollution deaths due to coal plant pollution (millions)
China	895.72	1.440
India	392.43	0.551
U.S.	157.02	0.021
Germany	60.96	0.020
Indonesia	43.17	0.017
World	2,319.04	2.407

Earlier studies on health effects of coal-fired power generation vary to a large degree. Vohra et al. (2021) documents 10.2 million global excess deaths per year are due to $PM_{2.5}$ from fossil fuel combustion. In the U.S., 350,000 premature deaths are attributed to emissions from the fossil sector. The number in India is 2.5 million people per year, representing over 30% of all-cause deaths. Penney et al. (2009) estimates 6,000 to 10,700 annual deaths are attributed to 88 publicly-financed coal power plants worldwide. Cropper et al. (2021) conclude that 112,000 deaths are attributable annually to coal-fired power plants in India. Lueken et al. (2016) finds between 7,500 and 52,000 people in the U.S. could be saved if switching from all coal plants to gas, equivalent to between $20 billion and $50 billion in monetized benefits. In Europe, Kushta et al. (2021) identifies 18,400-105,900 deaths are avoided from the phase-out of coal

power plants' emissions. In Africa, Marais et al. (2019) show 48,000 premature deaths due to fossil fuel electricity generation. Results in our paper lie in the wide range of previous estimates, and are slightly larger than most of the values, probably due to assuming all particles as $PM_{2.5}$. Our findings indicate the significant share of coal-fired power plants in pollution-caused deaths.

S2 Sensitivity checks

S2.1 'Strategic' location choice

Table S2.1: Alternative angle, using 30° to define wind directions

	ln(SO_2)	ln(GDP per capita)	ln(GDP)	ln(HDI)
	(1)	(2)	(3)	(4)
Downwind	0.156***	-0.031**	-0.022	-0.002**
	(0.012)	(0.014)	(0.017)	(0.001)
ln(Population)			0.966***	
			(0.015)	
Observations	905860	905860	905860	905860
R-square	0.041	0.000	0.811	0.000
Downwind	0.155***	-0.023***	-0.041***	-0.001**
	(0.012)	(0.008)	(0.015)	(0.001)
ln(Population)			1.152***	
			(0.019)	
Observations	905860	905860	905860	905860
R-square	0.374	0.965	0.950	0.964
Y-mean	0.282	8.789	17.794	0.511
Y-sd	0.383	0.828	2.251	0.060
Plant FEs	Y	Y	Y	Y

Notes: Standard errors are clustered at the plant level.

Table S2.2: Alternative distance, using 0.3-degree around plants

	ln(SO_2)	ln(GDP per capita)	ln(GDP)	ln(HDI)
	(1)	(2)	(3)	(4)
Downwind	0.211***	-0.031**	-0.032	-0.002**
	(0.011)	(0.012)	(0.020)	(0.001)
ln(Population)			0.988***	
			(0.019)	
Observations	498187	498187	498187	498187
R-square	0.064	0.000	0.799	0.000
Y-mean	0.404	8.812	17.952	0.512
Y-sd	0.417	0.837	2.325	0.060
Downwind	0.213***	-0.006	-0.019	-0.000
	(0.011)	(0.006)	(0.018)	(0.000)
ln(Population)			1.203***	

			(0.026)	
Observations	498187	498187	498187	498187
R-square	0.512	0.979	0.941	0.978
Y-mean	0.404	8.812	17.952	0.512
Y-sd	0.417	0.837	2.325	0.060
Plant FEs	Y	Y	Y	Y

Notes: Standard errors are clustered at the plant level.

S2.2 Does air pollution cause poverty?

Table S2.3: Alternative angle, using 30° to define wind directions

	$\ln(SO_2)$	ln(GDP per capita)	ln(GDP)	ln(HDI)
	(1)	(2)	(3)	(4)
Operating	0.025***	0.074***	0.064***	0.002***
	(0.007)	(0.010)	(0.011)	(0.000)
Downwind	-0.068***	0.001	-0.000	-0.000
	(0.005)	(0.003)	(0.004)	(0.000)
Operating × Downwind	0.174***	-0.003	0.001	0.000
	(0.013)	(0.006)	(0.009)	(0.000)
Observations	23552360	23552360	23552360	23552360
R-square	0.879	0.948	0.972	0.977
Y-mean	0.360	8.551	17.544	0.492
Y-sd	0.707	0.993	2.305	0.072
Pixel FEs	Y	Y	Y	Y
Year FEs	Y	Y	Y	Y

Notes: Standard errors are clustered at the plant level.

Table S2.4: Alternative distance, using 0.3-degree around plants

	$\ln(SO_2)$	ln(GDP per capita)	ln(GDP)	ln(HDI)
	(1)	(2)	(3)	(4)
Operating	0.094***	0.082***	0.073***	0.003***
	(0.010)	(0.010)	(0.012)	(0.001)
Downwind	-0.102***	0.001	-0.002	-0.000
	(0.007)	(0.002)	(0.005)	(0.000)
Operating × Downwind	0.264***	-0.004	0.006	0.000
	(0.015)	(0.006)	(0.012)	(0.000)
Observations	12952862	12952862	12952862	12952862
R-square	0.874	0.948	0.965	0.977
Y-mean	0.497	8.575	17.704	0.493
Y-sd	0.822	1.002	2.372	0.073
Pixel FEs	Y	Y	Y	Y
Year FEs	Y	Y	Y	Y

Notes: Standard errors are clustered at the plant level.

S2.3 Coexistence of pollution and poverty

Table S2.5: Summary statistics on refined samples

	Original sample	Refined 1	Refined 2	Refined 3
#Pixels	11,163,331	6,695,940	5,352,553	3,659,278
Average SO_2	0.493	0.583	0.688	0.919
Std.dev.	1.790	1.952	2.115	2.422
90 percentile	0	0.952	2.496	7.467

Table S2.6: SO_2 and GDP per capita using refined samples

	Panel A: ln(SO_2) and ln(GDP per capita)			
	Sample: Refined 1			
	(1)	(2)	(3)	(4)
ln(GDP per capita)	0.029	1.604	-0.236	-10.616*
	(0.089)	(0.982)	(5.260)	(6.154)
ln(GDP per capita)^2		-0.084	0.115	1.188*
		(0.052)	(0.571)	(0.676)
ln(GDP per capita)^3			-0.007	-0.043*
			(0.020)	(0.024)
Observations	6695940	6695940	6695940	6695940
R-square	0.000	0.005	0.005	0.146
Y-mean	0.583	0.583	0.583	0.583
Y-sd	1.952	1.952	1.952	1.952
	Panel B: ln(SO_2) and ln(GDP per capita)			
	Sample: Refined 2			
ln(GDP per capita)	-0.050	1.544	2.798	-11.828
	(0.121)	(0.983)	(5.958)	(7.351)
ln(GDP per capita)^2		-0.084	-0.219	1.320
		(0.052)	(0.652)	(0.806)
ln(GDP per capita)^3			0.005	-0.048
			(0.023)	(0.029)
Observations	5352553	5352553	5352553	5352553
R-square	0.000	0.004	0.004	0.136
Y-mean	0.688	0.688	0.688	0.688
Y-sd	2.115	2.115	2.115	2.115
	Panel C: ln(SO_2) and ln(GDP per capita)			
	Sample: Refined 3			
ln(GDP per capita)	-0.209**	1.515	5.580	-14.072
	(0.090)	(1.844)	(8.290)	(11.489)
ln(GDP per capita)^2		-0.087	-0.506	1.599
		(0.092)	(0.880)	(1.252)
ln(GDP per capita)^3			0.014	-0.058
			(0.031)	(0.044)
Observations	3659278	3659278	3659278	3659278
R-square	0.005	0.008	0.008	0.117
Y-mean	0.919	0.919	0.919	0.919

Y-sd	2.422	2.422	2.422	2.422
Country FEs				Y

Notes: Unit of SO_2: nano gram/m^3, unit of GDP and GDP per capita: constant 2011 international US dollar. Standard errors are clustered at the country level.

Table S2.7: SO_2 and GDP using refined samples

	Panel A: ln(SO_2) and ln(GDP) Sample: Refined 1			
	(1)	(2)	(3)	(4)
ln(GDP)	0.118***	-0.862***	0.844	1.129***
	(0.038)	(0.254)	(0.572)	(0.407)
$\ln(GDP)^2$		0.033***	-0.082*	-0.096***
		(0.010)	(0.044)	(0.033)
$\ln(GDP)^3$			0.003**	0.003***
			(0.001)	(0.001)
ln(Population)	0.153***	0.104***	0.112***	0.144***
	(0.046)	(0.032)	(0.034)	(0.041)
R-square	0.104	0.126	0.127	0.205
	Panel B: ln(SO_2) and ln(GDP) Sample: Refined 2			
ln(GDP)	0.106**	-0.885***	0.874	1.037**
	(0.040)	(0.256)	(0.646)	(0.454)
$\ln(GDP)^2$		0.034***	-0.085*	-0.091**
		(0.010)	(0.049)	(0.036)
$\ln(GDP)^3$			0.003**	0.003**
			(0.001)	(0.001)
ln(Population)	0.205***	0.147***	0.157***	0.163***
	(0.048)	(0.033)	(0.036)	(0.045)
R-square	0.121	0.140	0.142	0.203
	Panel C: ln(SO_2) and ln(GDP) Sample: Refined 3			
ln(GDP)	0.148**	-1.080***	1.257	1.463**
	(0.059)	(0.229)	(0.835)	(0.583)
$\ln(GDP)^2$		0.042***	-0.114*	-0.125**
		(0.009)	(0.060)	(0.044)
$\ln(GDP)^3$			0.003**	0.003***
			(0.001)	(0.001)
ln(Population)	0.232***	0.163***	0.177***	0.234***
	(0.059)	(0.042)	(0.044)	(0.044)
R-square	0.144	0.165	0.167	0.210
Country FEs				Y

Notes: Unit of SO_2: nano gram/m^3, unit of GDP and GDP per capita: constant 2011 international US dollar. Standard errors are clustered at the country level.

Table S2.8: SO_2 and HDI using refined samples

	Panel A: ln(SO_2) and ln(HDI) Sample: Refined 1			
	(1)	(2)	(3)	(4)
ln(HDI)	0.905	-0.316	-51.708	-337.796
	(1.606)	(27.775)	(133.311)	(220.414)
$\ln(HDI)^2$		1.131	98.098	650.791
		(25.468)	(257.632)	(422.278)
$\ln(HDI)^3$			-60.203	-406.628
			(165.204)	(263.778)
R-square	0.001	0.001	0.001	0.151
	Panel B: ln(SO_2) and ln(HDI) Sample: Refined 2			
ln(HDI)	-0.549	-23.676	-154.370	-541.779*
	(2.319)	(36.339)	(210.878)	(314.125)
$\ln(HDI)^2$		20.950	264.496	1038.392*
		(33.076)	(398.364)	(596.010)
$\ln(HDI)^3$			-149.504	-649.310*
			(249.063)	(370.308)
R-square	0.000	0.002	0.003	0.143
	Panel C: ln(SO_2) and ln(HDI) Sample: Refined 3			
ln(HDI)	-1.240	-10.249	-51.463	-796.260*
	(2.976)	(42.751)	(324.803)	(373.603)
$\ln(HDI)^2$		8.296	85.102	1522.164**
		(38.847)	(625.054)	(706.029)
$\ln(HDI)^3$			-47.142	-950.258**
			(395.360)	(437.931)
R-square	0.001	0.001	0.001	0.128
Country FEs				Y

Notes: Unit of SO_2: nano gram/m^3, unit of GDP and GDP per capita: constant 2011 international US dollar. Standard errors are clustered at the country level.

Table S2.9: SO_2 and income using pixels within 2-degree of any plant

	Panel A: ln(SO_2) and ln(GDP per capita) Sample: Pixels near plants			
	(1)	(2)	(3)	(4)
ln(GDP per capita)	0.213**	2.513	-1.664	-15.360**
	(0.092)	(2.135)	(8.253)	(6.260)
$\ln(\text{GDP per capita})^2$		-0.121	0.332	1.725**
		(0.114)	(0.962)	(0.682)
$\ln(\text{GDP per capita})^3$			-0.016	-0.063**
			(0.037)	(0.024)
Observations	3755823	3755823	3755823	3755823
R-square	0.005	0.007	0.007	0.086
Y-mean	1.386	1.386	1.386	1.386

Y-sd	2.798	2.798	2.798	2.798
	Panel B: ln(SO_2) and ln(GDP)			
	Sample: Pixels near plants			
ln(GDP)	0.239***	-0.648***	0.066	0.738
	(0.045)	(0.232)	(0.836)	(0.695)
$\ln(GDP)^2$		0.028***	-0.017	-0.058
		(0.007)	(0.060)	(0.050)
$\ln(GDP)^3$			0.001	0.002
			(0.001)	(0.001)
ln(Population)	0.081	0.049	0.052	0.228***
	(0.074)	(0.065)	(0.068)	(0.040)
R-square	0.073	0.080	0.081	0.146
	Panel C: ln(SO_2) and ln(HDI)			
	Sample: Pixels near plants			
ln(HDI)	2.748*	12.632	-188.343	-353.364**
	(1.520)	(29.239)	(139.286)	(148.676)
$\ln(HDI)^2$		-8.926	367.110	672.963**
		(26.236)	(264.072)	(276.158)
$\ln(HDI)^3$			-231.182	-416.849**
			(166.568)	(167.551)
R-square	0.004	0.005	0.006	0.087
Country FEs				Y

Notes: Unit of SO_2: nano gram/m^3, unit of GDP and GDP per capita: constant 2011 international US dollar. Standard errors are clustered at the country level.

S3 Reduced form tables

Table S3.1: Reduced form results

	Panel A: ln(GDP per capita)			
	(1)	(2)	(3)	(4)
Operating	0.977***	0.905***	0.469***	0.075***
	(0.033)	(0.014)	(0.064)	(0.009)
Downwind	-0.033**	-0.005	-0.034***	0.001
	(0.013)	(0.010)	(0.013)	(0.002)
Operating × Downwind	0.010	0.001	0.007	-0.003
	(0.012)	(0.006)	(0.012)	(0.006)
Observations	34971846	34971846	34971846	34971846
R-square	0.232	0.829	0.313	0.948
Y-mean	8.563	8.563	8.563	8.563
Y-sd	1.002	1.002	1.002	1.002
	Panel B: ln(GDP)			
Operating	1.074***	0.972***	0.534***	0.064***
	(0.037)	(0.014)	(0.068)	(0.010)
Downwind	0.023	-0.008	0.021	-0.001
	(0.033)	(0.011)	(0.033)	(0.003)
Operating × Downwind	0.003	0.008	0.000	0.003
	(0.028)	(0.009)	(0.028)	(0.008)
ln(Population)	0.854***	0.000	0.853***	0.000
	(0.018)	(.)	(0.018)	(.)
Observations	34971846	34971846	34971846	34971846
R-square	0.474	0.944	0.491	0.971
Y-mean	17.534	17.534	17.534	17.534
Y-sd	2.337	2.337	2.337	2.337
	Panel C: ln(HDI)			
Operating	0.071***	0.065***	0.032***	0.002***
	(0.002)	(0.001)	(0.005)	(0.000)
Downwind	-0.003***	-0.001	-0.003***	-0.000
	(0.001)	(0.001)	(0.001)	(0.000)
Operating × Downwind	0.002*	0.001*	0.001	0.000
	(0.001)	(0.000)	(0.001)	(0.000)
Observations	34971846	34971846	34971846	34971846
R-square	0.232	0.840	0.327	0.977
Y-mean	0.493	0.493	0.493	0.493
Y-sd	0.073	0.073	0.073	0.073
Pixel FEs		Y		Y
Year FEs			Y	Y

Notes: Standard errors are clustered at the plant level.

Table S3.2: Heterogeneity by plant start year

	Panel A: old plants (1992-2007)			
	$\ln(SO_2)$	ln(GDP per capita)	ln(GDP)	ln(HDI)

	(1)	(2)	(3)	(4)
Operating	0.025**	0.101***	0.094***	0.005***
	(0.010)	(0.015)	(0.016)	(0.001)
Downwind	-0.081***	0.000	-0.003	-0.000
	(0.009)	(0.005)	(0.006)	(0.000)
Operating × Downwind	0.153***	0.001	0.007	0.000
	(0.015)	(0.008)	(0.010)	(0.000)
Observations	19441994	19441994	19441994	19441994
R-square	0.873	0.949	0.967	0.973
Y-mean	0.365	8.667	17.757	0.503
Y-sd	0.697	1.053	2.306	0.074
	Panel B: new plants (2008-2013)			
Operating	0.027**	0.117***	0.099***	0.002**
	(0.013)	(0.024)	(0.025)	(0.001)
Downwind	-0.033***	0.002	0.000	-0.000
	(0.004)	(0.002)	(0.003)	(0.000)
Operating × Downwind	0.158***	-0.012	-0.004	0.000
	(0.017)	(0.008)	(0.016)	(0.000)
Observations	15529852	15529852	15529852	15529852
R-square	0.885	0.946	0.974	0.981
Y-mean	0.323	8.432	17.256	0.480
Y-sd	0.683	0.918	2.347	0.070
Pixel FEs	Y	Y	Y	Y
Year FEs	Y	Y	Y	Y

Notes: Standard errors are clustered at the plant level.

Table S3.3: Heterogeneity by plant country's income

	Panel A: rich quartile			
	ln(SO_2)	ln(GDP per capita)	ln(GDP)	ln(HDI)
	(1)	(2)	(3)	(4)
Operating	0.029***	0.019*	0.022	0.002**
	(0.008)	(0.011)	(0.016)	(0.001)
Downwind	-0.071***	-0.002	-0.006	-0.000
	(0.010)	(0.005)	(0.011)	(0.000)
Operating × Downwind	0.141***	0.002	0.010	0.001
	(0.018)	(0.011)	(0.024)	(0.001)
Observations	6308380	6308380	6308380	6308380
R-square	0.956	0.971	0.964	0.979
Y-mean	0.464	10.010	17.741	0.585
Y-sd	0.809	0.742	2.735	0.063
	Panel B: poor quartile			
Operating	0.014	0.022*	0.020	-0.001
	(0.017)	(0.013)	(0.017)	(0.001)
Downwind	-0.054***	0.002	0.006	-0.000
	(0.009)	(0.003)	(0.005)	(0.000)
Operating × Downwind	0.192***	-0.005	-0.019	0.001
	(0.029)	(0.011)	(0.017)	(0.001)

Observations	4990440	4990440	4990440	4990440
R-square	0.916	0.954	0.965	0.991
Y-mean	0.479	7.947	17.414	0.428
Y-sd	0.921	0.526	1.846	0.069
Pixel FEs	Y	Y	Y	Y
Year FEs	Y	Y	Y	Y

Notes: Standard errors are clustered at the plant level.

Table S3.4: Heterogeneity by plant country's pollution

	Panel A: polluting quartile			
	$\ln(SO_2)$	ln(GDP per capita)	ln(GDP)	ln(HDI)
	(1)	(2)	(3)	(4)
Operating	0.029**	0.009	0.006	-0.001
	(0.013)	(0.010)	(0.015)	(0.001)
Downwind	-0.079***	-0.004	0.003	-0.001***
	(0.009)	(0.003)	(0.005)	(0.000)
Operating × Downwind	0.217***	0.012	-0.009	0.002***
	(0.024)	(0.010)	(0.015)	(0.000)
Observations	7165002	7165002	7165002	7165002
R-square	0.932	0.987	0.973	0.990
Y-mean	0.622	8.769	17.637	0.490
Y-sd	0.991	1.130	2.088	0.103
	Panel B: clean quartile			
Operating	0.039***	0.065***	0.049*	0.002*
	(0.008)	(0.021)	(0.028)	(0.001)
Downwind	-0.029***	-0.001	-0.021	-0.000
	(0.006)	(0.006)	(0.014)	(0.000)
Operating × Downwind	0.072***	0.003	0.052	0.001
	(0.012)	(0.015)	(0.033)	(0.001)
Observations	4133818	4133818	4133818	4133818
R-square	0.936	0.980	0.953	0.981
Y-mean	0.209	9.672	17.528	0.560
Y-sd	0.460	1.144	2.835	0.083
Pixel FEs	Y	Y	Y	Y
Year FEs	Y	Y	Y	Y

Notes: Standard errors are clustered at the plant level.

S4 Additional figures

Figure S4.1: Global analysis at the country level: #plants and income

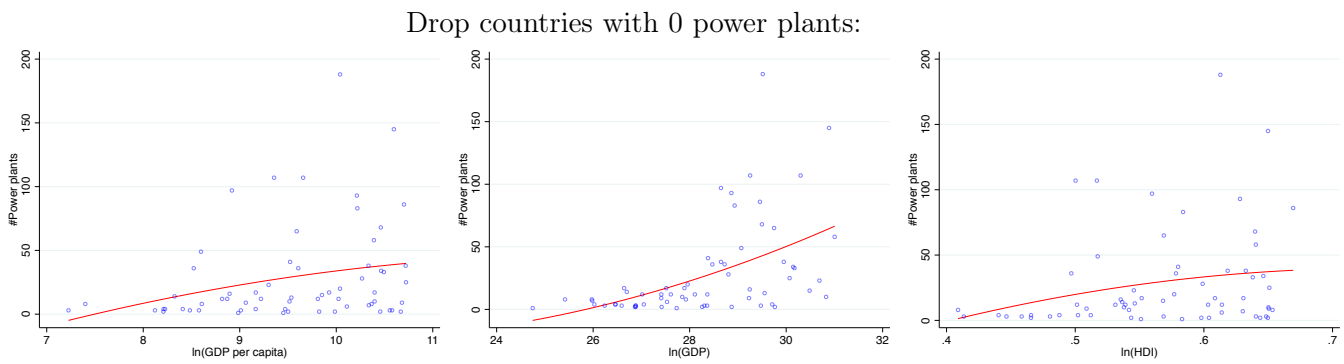

Figure S4.2: Event study figures: pollution and GDP, HDI